

Nonparametric predictive inference for discrete data via Metropolis-adjusted Dirichlet sequences

Davide Agnoletto¹, Tommaso Rigon², and David B. Dunson¹

¹Department of Statistical Science, Duke University, Durham, NC, USA

²Department of Economics, Management, and Statistics, University of Milano–Bicocca, 20126
Milano, Italy

Abstract

This article is motivated by challenges in conducting Bayesian inferences on unknown discrete distributions, with a particular focus on count data. To avoid the computational disadvantages of traditional mixture models, we develop a novel Bayesian predictive approach. In particular, our Metropolis-adjusted Dirichlet (MAD) sequence model characterizes the predictive measure as a mixture of a base measure and Metropolis-Hastings kernels centered on previous data points. The resulting MAD sequence is asymptotically exchangeable and the posterior on the data generator takes the form of a martingale posterior. This structure leads to straightforward algorithms for inference on count distributions, with easy extensions to multivariate, regression, and binary data cases. We obtain a useful asymptotic Gaussian approximation and illustrate the methodology on a variety of applications.

Keywords: Count data; Martingale posterior; Nonparametric Bayes; Predictive inference; Smoothing

1 INTRODUCTION

Bayesian nonparametric modeling of count distributions is a challenging task, and several solutions have been proposed over the years. A Bayesian nonparametric mixture of Poisson kernels lacks flexibility since both centering and scaling of the kernels are controlled by a single parameter. [Canale and Dunson \(2011\)](#), [Canale and Prünster \(2017\)](#) proposed a more flexible class of kernels obtained by rounding continuous distributions. However, estimating these mixture models using Markov chain Monte Carlo (MCMC) algorithms can be cumbersome in practice. Alternatively, one can directly specify a Dirichlet process (DP) prior ([Ferguson, 1973](#)) on the data generator as

$$Y_i \mid P \stackrel{\text{iid}}{\sim} P, \quad P \sim \text{DP}(\alpha, P_0), \quad (1)$$

where $Y_i \in \mathcal{Y}$, $i = 1, \dots, n$, are assumed to be independent and identically distributed (iid) conditionally on P , \mathcal{Y} is a countable space, α is the precision parameter, and P_0 is a base parametric distribution, such as a Poisson. Despite the appealing flexibility, it is well known that assuming (1) produces the conjugate posterior distribution

$$P \mid y_{1:n} \sim \text{DP}\left(\alpha + n, P_0 + \sum_{i=1}^n \delta_{y_i}\right),$$

with $y_{1:n} = (y_1, \dots, y_n)$, which lacks smoothing and therefore tends to have poor performance unless the distribution is concentrated on a small number of values. However, using traditional Bayesian nonparametric machinery, it is not clear how to specify a nonparametric process P having the same simplicity and flexibility as (1) while allowing smoothing. This motivates taking a predictive approach, which bypasses the need to directly specify a prior for P .

In a predictive approach, the statistical uncertainty is taken into account by modeling the conditional distribution of new data Y_{n+1} given past observations $y_{1:n}$. Blackwell and MacQueen (1973) described the predictive rule resulting from the DP prior using a Pólya urn scheme for which $Y_1 \sim P_0$ and $Y_{n+1} \mid y_{1:n} \sim P_n$ for $n \geq 1$, where

$$P_n(A) = \mathbb{P}(Y_{n+1} \in A \mid y_{1:n}) = \frac{\alpha}{\alpha + n} P_0(A) + \frac{1}{\alpha + n} \sum_{i=1}^n \mathbf{1}(y_i \in A), \quad (2)$$

for any measurable set $A \subseteq \mathcal{Y}$ and where $\mathbf{1}(\cdot)$ denotes the indicator function. The sequence $(Y_n)_{n \geq 1}$ generated according to (2) is known as a Dirichlet sequence and is a conditionally iid random sample from P , with $P \sim \text{DP}(\alpha, P_0)$. Although predictive laws can be obtained by marginalizing models of the form in (1), potentially with alternative priors used in place of the DP, we instead start by defining the predictive law P_n . Thanks to Ionescu-Tulcea's theorem one can characterize the law of the joint sequence $(Y_n)_{n \geq 1}$ by specifying a sequence of one-step-ahead predictive distributions. Moreover, if the resulting sequence is exchangeable, de Finetti's theorem implies the existence of a random probability measure P , conditionally on which the data are iid. This strategy bypasses prior elicitation; in our case, avoiding the difficult problem of directly specifying a prior for P . Moreover, it highlights how the tasks of inference and prediction are intrinsically connected within the Bayesian paradigm. There is a growing recent literature discussing the foundations of the Bayesian predictive approach, see for example Fortini and Petrone (2012, 2023, 2025), Holmes and Walker (2023), Fong et al. (2023), Berti et al. (2025).

It is reasonable to think that a better estimator for count data distributions would be obtained by replacing $\mathbf{1}(\cdot)$ in (2) with a more diffuse kernel that allows the borrowing of information between the atoms. Early ideas along these lines can be found in Hjort (1994a,b), whereas Berti et al. (2023b) provide a rigorous recent discussion. Unfortunately, for a general choice of the kernel, the corresponding sequence of predictive distributions does not generate an exchangeable sequence of random variables

(Sariev and Savov, 2024), which is required for recovering the posterior distribution through de Finetti’s theorem. To address this problem, we consider a generalization of the predictive approach that relaxes the exchangeability assumption.

In this paper, we introduce a novel generalized Bayesian predictive method to model count data distributions. We propose the recursive predictive rule

$$P_n(A) = (1 - w_n)P_{n-1}(A) + w_n K_n(A \mid y_n), \quad (3)$$

for any measurable set $A \subseteq \mathcal{Y}$, where $(w_n)_{n \geq 1}$ is a sequence of decreasing weights $w_n \in (0, 1)$, and, for all $n \geq 1$ we let $K_n(\cdot \mid y_n) = K(\cdot; y_n, P_{n-1})$ be a sequence of Metropolis-Hastings (MH) kernels, which will be formally defined in Section 2. The special case (2) is recovered for $w_n = (\alpha + n)^{-1}$ and $K_n(\cdot \mid y_n) = \mathbb{1}(y_n \in \cdot)$. The simple structure (3) resembles a frequentist kernel density estimator (KDE, Wand and Jones, 1995) under a particular choice of weights w_n , where MH kernels centered at the observed data points serve a similar role to local kernels in KDE. More precisely, if $w_n = (\alpha + n)^{-1}$, then the recursion in equation (3) becomes

$$P_n(A) = \frac{\alpha}{\alpha + n} P_0(A) + \frac{1}{\alpha + n} \sum_{i=1}^n K_i(A \mid y_i).$$

This is similar in spirit to the recursive predictive algorithms of Hahn et al. (2018); Fong et al. (2023), but, crucially, we specify a kernel $K_n(\cdot \mid y_n)$ tailored for count data. The predictive rule (3) with MH kernels generates a Metropolis-adjusted Dirichlet (MAD) sequence, which we show to be conditionally identically distributed (CID, Kallenberg, 1988; Berti et al., 2004). In particular, MADs are CID sequences admitting a recursive structure (Berti et al., 2023a). Consequently, MAD sequences are asymptotically exchangeable, which means that, for large n , $(Y_n)_{n \geq 1}$ can be regarded as an approximately iid sample from a random distribution P . In other words, the predictive (3) implies the existence of an implicit prior for P , which is a novel alternative to a DP. The posterior of P can be regarded as a martingale posterior in the sense of Fong et al. (2023), implying that a predictive resampling algorithm can be used to obtain posterior samples for P allowing uncertainty quantification.

The literature about CID sequences (e.g. Berti et al., 2004, 2012; Fortini et al., 2018; Berti et al., 2021, 2023a, 2025) has strong roots in probability theory, but the statistical properties of such sequences have not been fully investigated, with a few notable exceptions. An approach based on the direct specification of copulas is discussed in Hahn et al. (2018); Fong et al. (2023), whose focus is on continuous data with a Gaussian copula; see also Cui and Walker (2024); Fong and Yiu (2024b); Bissiri and Walker (2025) for related works. Such an update is not designed for count data, and when modeling multivariate distributions, it is dimension ordering dependent. As an alternative, Fortini and Petrone (2020) provided a Bayesian interpretation for the popular Newton recursive density estimator (Newton and Zhang, 1999; Newton, 2002) and proved that the resulting sequence is CID. Although, in principle, the Newton

estimator can be adapted to the discrete case, the algorithm requires a numerical evaluation of an integral at each step, which could lead to computational bottlenecks if a closed form is not available; using (3) is substantially simpler.

We argue that employing MH kernels is particularly convenient for modeling count distributions for several reasons. First, these kernels offer a clear interpretation as a mixture of an arbitrary kernel centered on past data and the DP update, which is recovered as a special case. This structure enables the borrowing of information between nearby values in the support when updating the predictive rule, resulting in a smoother estimator than the DP. Second, computing the MAD predictive is easy in practice, which is crucial since (3) represents the posterior mean of P . Consequently, obtaining a point estimate is efficient and does not require predictive resampling nor MCMC. Third, the properties of the kernel facilitate extensions to the multivariate case and nonparametric regression, as the update remains invariant to the ordering of dimensions. This approach is also suitable for modeling multivariate binary data and proves particularly effective for nonparametric regression with binary covariates, as demonstrated through simulations and real data analyses. Moreover, we obtain an asymptotic Gaussian approximation for the posterior distribution of P , highlighting the roles of the weights w_n and the kernel bandwidth in the learning mechanism.

2 METROPOLIS-ADJUSTED DIRICHLET SEQUENCES

We introduce a novel nonparametric predictive framework for modeling count data. Our goal is to develop a predictive construction that preserves the simplicity and flexibility of the Pólya urn scheme, while allowing for borrowing of information between atoms. Let $(Y_n)_{n \geq 1}$ be a sequence of random variables defined on a countable space \mathcal{Y} . In the proposed approach, we assume that

$$Y_1 \sim P_0, \quad \text{and} \quad Y_{n+1} \mid y_{1:n} \sim P_n, \quad (4)$$

for $n \geq 1$, with $P_n(\cdot) = \mathbb{P}(Y_{n+1} \in \cdot \mid y_{1:n})$ defined as in (3) for some sequence of decreasing weights $(w_n)_{n \geq 1}$. In practice, we require $\sum_{n \geq 1} w_n = \infty$ and $\sum_{n \geq 1} w_n^2 < \infty$ as this ensures good frequentist properties (Fortini and Petrone, 2020; Fong et al., 2023), although this is not necessary to guarantee that $(Y_n)_{n \geq 1}$ is CID. The weights $w_n = (\alpha + n)^{-\lambda}$, with $\alpha > 0$ and $\lambda \in (0.5, 1]$, satisfy the required conditions. Importantly, this sequential construction leads to a unique and well-defined joint distribution \mathbb{P} for the entire sequence $(Y_n)_{n \geq 1}$ thanks to the celebrated Ionescu–Tulcea theorem (e.g. Berti et al., 2025), which serves as the mathematical foundation of the predictive approach. To streamline the notation, we use capital letters P_0 , $P_n(\cdot)$, and $K_n(\cdot \mid y_n)$ to denote probability measures, and lowercase $p_0(y)$, $p_n(y)$, and $k_n(y \mid y_n)$ for their corresponding probability mass functions. This convention will be used consistently throughout the paper.

Definition 1. Let \mathcal{Y} be a countable space and consider the recursive predictive rule (3) for $n \geq 1$

$$p_n(y) = (1 - w_n)p_{n-1}(y) + w_n k_n(y | y_n), \quad y \in \mathcal{Y},$$

with initial distribution $p_0(y)$ and weights $w_n \in (0, 1)$. The Metropolis-Hastings kernel is defined as

$$k_n(y | y_n) = \gamma_n(y, y_n) k_*(y | y_n) + \mathbf{1}(y = y_n) \left[1 - \sum_{z \in \mathcal{Y}} \gamma_n(z, y_n) k_*(z | y_n) \right], \quad (5)$$

where $k_*(y | y_n)$ is a discrete base kernel and $\gamma_n(y, y_n)$ is a probability weight defined as

$$\gamma_n(y, y_n) = \gamma(y, y_n, p_{n-1}) = \min \left\{ 1, \frac{p_{n-1}(y) k_*(y_n | y)}{p_{n-1}(y_n) k_*(y | y_n)} \right\}. \quad (6)$$

The predictive distribution p_n is referred to as the Metropolis-adjusted Dirichlet (MAD) distribution with weights $(w_n)_{n \geq 1}$, base kernel k_* , and initial distribution p_0 . The corresponding sequence of random variables $(Y_n)_{n \geq 1}$, as defined in (4), is called a MAD sequence.

The kernel probability mass function (5) can be interpreted as a mixture of a re-weighted discrete base kernel and a point mass at y_n . Specifically, for each $y \in \mathcal{Y}$, the base kernel probability $k_*(y | y_n)$ is weighted by $\gamma_n(y, y_n)$, which reflects how well it aligns with $p_{n-1}(y)$, as defined in (6). Since $\sum_{y \in \mathcal{Y}} \gamma_n(y, y_n) k_*(y | y_n) \leq 1$, the remaining probability mass is assigned to y_n . When $\gamma_n(y, y_n) = 0$ for every $y \in \mathcal{Y}$, we obtain $k_n(y | y_n) = \mathbf{1}(y = y_n)$, and the DP predictive distribution is recovered if $w_n = (\alpha + n)^{-1}$. At the other extreme, when $\gamma_n(y, y_n) = 1$ for every $y \in \mathcal{Y}$, we obtain $k_n(y | y_n) = k_*(y | y_n)$. For intermediate values of $\gamma_n(y, y_n)$, the MH kernel adjusts the Polya-urn scheme, introducing a smooth deviation from the DP update. This flexibility makes MAD sequences particularly appealing for modeling discrete distributions.

2.1 BAYESIAN PROPERTIES OF MAD SEQUENCES

We provide a formal Bayesian justification for using a MAD sequence to model discrete data. Although MAD sequences are not exchangeable, they are conditionally identically distributed (CID). The notion of CID sequences was introduced by [Kallenberg \(1988\)](#) as a relaxation of exchangeability, and it has been further developed by [Berti et al. \(2004\)](#). A sequence $(Y_n)_{n \geq 1}$ of random variables is said to be CID if $\mathbb{P}(Y_n \in \cdot) = P_0(\cdot)$ for every $n \geq 1$, meaning that each Y_n has the same marginal distribution P_0 a priori, and

$$\mathbb{P}(Y_{n+k} \in \cdot | y_{1:n}) = \mathbb{P}(Y_{n+1} \in \cdot | y_{1:n}) = P_n(\cdot), \quad \text{for all } k \geq 1, n \geq 1. \quad (7)$$

It is sufficient to verify this condition for $k = 1$ in order to ensure its validity for all $k \geq 1$. Equivalently, [Fong et al. \(2023\)](#) express condition (7) in a way that emphasizes the martingale property of the predictive distributions $(P_n)_{n \geq 1}$:

$$\mathbb{E}\{P_{n+1}(\cdot) | y_{1:n}\} = P_n(\cdot), \quad n \geq 1. \quad (8)$$

Note that $\mathbb{E}\{P_{n+1}(\cdot) \mid y_{1:n}\} = \mathbb{P}(Y_{n+2} \in \cdot \mid y_{1:n})$, which highlights the equivalence between the martingale and CID conditions. See [Berti et al. \(2012, Theorem 3.1\)](#) for a formal proof.

Theorem 1. *Let $(Y_n)_{n \geq 1}$ be a MAD sequence. Then, for every choice of weight sequence $(w_n)_{n \geq 1}$, discrete base kernel k_* , and initial distribution p_0 , the sequence $(Y_n)_{n \geq 1}$ is CID.*

Theorem 1 follows as a special case of [Berti et al. \(2023a, Theorem 2\)](#), since MAD sequences fall within the broad class of predictive updates based on stationary kernels. Let $\theta = P(f) = \sum_{y \in \mathcal{Y}} f(y)p(y)$ denote any functional of interest, and analogously let $\theta_n = P_n(f) = \sum_{y \in \mathcal{Y}} f(y)p_n(y)$ denote its predictive counterpart.

Corollary 1 ([Berti et al., 2004](#)). *Consider a MAD sequence $(Y_n)_{n \geq 1}$. Then, \mathbb{P} -a.s.,*

(a) *The sequence is asymptotically exchangeable, that is*

$$(Y_{n+1}, Y_{n+2}, \dots) \xrightarrow{d} (Z_1, Z_2, \dots), \quad n \rightarrow \infty,$$

where (Z_1, Z_2, \dots) is an exchangeable sequence with directing random probability measure P ;

(b) *The corresponding sequence predictive distributions $(P_n)_{n \geq 1}$ and empirical distributions $(\hat{P}_n)_{n \geq 1}$, where $\hat{P}_n := n^{-1} \sum_{i=1}^n \delta_{Y_i}$, converge weakly to the random probability measure P ;*

(c) *For every $n \geq 1$ and every integrable function $f : \mathcal{Y} \rightarrow \mathbb{R}$, we have $\mathbb{E}(\theta) = \theta_0$ and $\mathbb{E}(\theta \mid y_{1:n}) = \theta_n$.*

These results ensure that MAD sequences are a valid Bayesian method for nonparametric inference, bypassing direct prior specification on the space of probability distributions. The results of Corollary 1 are based on the general results provided by [Berti et al. \(2004\)](#) for CID sequences. Although the probability law implied by a MAD sequence is not ordering-invariant, part (a) of Corollary 1 guarantees that this dependence vanishes asymptotically. As a result, for large n , exchangeability is recovered and, informally, we will say $Y_i \mid P \overset{\text{iid}}{\sim} P$ for large n . Thus, an asymptotic equivalent of de Finetti's theorem holds: each MAD sequence has a corresponding unique prior on P and part (b) guarantees that P is defined as the limit of the predictive distributions. This convergence holds in the weak sense, but it can be strengthened to total variation convergence (see Lemma A.1 in Appendix A). Finally, by part (c) we have $\theta = \mathbb{E}\{P(f)\} = P_0(f) = \theta_0$ for every integrable function f , so that P_0 retains the role of a base measure as for standard Dirichlet sequences, providing an initial guess at P . In particular, if $f(y) = \mathbb{1}_A(y)$ is the indicator function for some measurable $A \subseteq \mathcal{Y}$, then we get $\mathbb{E}\{P(A)\} = P_0(A)$. Consequently, prior or external information can still be incorporated into the model through P_0 . Theorem 1 and Corollary 1 are valid for a general sequence of weights $(w_n)_{n \geq 1}$. When $w_n = (\alpha + n)^{-\lambda}$, the parameter α retains the same interpretation as the precision parameter in the DP, controlling the degree of shrinkage of P toward P_0 . Setting large values for α denotes a strong

confidence in the base measure, while $\alpha = 1$ provides a useful weakly informative default value. For a discussion of the role of λ based on asymptotic considerations, we refer to Section 2.4.

Given the data $y_{1:n}$, the predictive distributions P_n converge to the posterior distribution for P , which can be considered a martingale posterior in the sense of Fong et al. (2023). Prior and posterior sampling of P can be performed using a simple Monte Carlo scheme (see Section 2.3). To illustrate, if the sequence of predictive distributions is equation (2), then the output of the posterior sampling algorithm for a given set $A \subseteq \mathcal{Y}$ would be an approximate iid sample from $P(A) \mid y_{1:n}$, whose distribution is

$$\text{Beta}\left(\alpha P_0(A) + \sum_{i=1}^n \mathbf{1}(y_i \in A), \alpha + n - \alpha P_0(A) - \sum_{i=1}^n \mathbf{1}(y_i \in A)\right),$$

that is, the distribution of $P(A) \mid y_{1:n}$ when assuming a DP prior. However, to obtain a point estimate for any functional of interest $\theta = P(f)$, sampling is not necessary. By part (c), the posterior mean is $\mathbb{E}(\theta \mid y_{1:n}) = \mathbb{E}\{P(f) \mid y_{1:n}\} = P_n(f) = \theta_n$, which is a consequence of the martingale property.

Although the posterior variance of $P(f)$ depends on the unknown limit distribution P , examining the variance of $P_{n+1}(f)$ given the observed data provides useful insights into MAD sequences. The expected variation in the predictive distribution after observing a new data point is expressed as

$$\text{var}\{P_{n+1}(f) \mid y_{1:n}\} = \mathbb{E}\{[P_{n+1}(f) - P_n(f)]^2 \mid y_{1:n}\} = w_{n+1}^2 \left\{ \sum_{y \in \mathcal{Y}} K_n(f \mid y) p_n(y) - P_n(f)^2 \right\}. \quad (9)$$

When no data are observed, (9) represents the expected prior-to-posterior variability after the first observation. We will show in Section 2.4 that the variance of P_{n+1} is also closely related to the asymptotic variance of P . Moreover, the correlation between two measurable functions f_1, f_2 induced by P_{n+1} given $y_{1:n}$ is

$$\begin{aligned} \text{cor}\{P_{n+1}(f_1), P_{n+1}(f_2) \mid y_{1:n}\} &= \\ &= \frac{\sum_{y \in \mathcal{Y}} K_n(f_1 \mid y) K_n(f_2 \mid y) p_n(y) - P_n(f_1) P_n(f_2)}{\sqrt{[\sum_{y \in \mathcal{Y}} K_n(f_1 \mid y) p_n(y) - P_n(f_1)^2] [\sum_{y \in \mathcal{Y}} K_n(f_2 \mid y) p_n(y) - P_n(f_2)^2]}}. \end{aligned} \quad (10)$$

Remark 1. In general, the predictive law P_n of a CID sequence depends on the order of the observations $y_{1:n}$, which is typically unappealing. In contrast, the predictive law P_n of an exchangeable sequence does not depend on the order of $y_{1:n}$ (Fortini et al., 2000). This raises the question of whether a CID sequence whose predictive distribution is order-invariant even exists. A profound and elegant answer is provided in Fortini et al. (2018, Corollary 3.7), which establishes that a CID sequence is exchangeable if and only if its predictive law does not depend on the ordering of the observations. In other words, order dependence in martingale posteriors is unavoidable—otherwise, we would revert to the classical exchangeable framework, which is often too restrictive.

2.2 ON THE CHOICE OF THE BASE KERNEL

In this section, we consider the univariate space $\mathcal{Y} = \{0, 1, \dots\}$, whereas in Section 3 we will address the multivariate case. Although the results in Section 2.1 hold for an arbitrary discrete base kernel k_* , the choice of kernel has important consequences for the MH update. For example, using Poisson base kernels—where a single parameter governs both the location and the scale—limits the flexibility of the MH kernel, as the same parameter simultaneously controls both the bandwidth and the center of the distribution. A simple alternative, resembling common choices in KDE, is to consider a uniform kernel over the interval $\{y_n - m, \dots, y_n + m\}$ for some $m \geq 0$, that is, $k_*(y \mid y_n, m) = (2m + 1)^{-1}$ if $y \in \{y_n - m, \dots, y_n + m\}$ and 0 otherwise. Then, the resulting MH kernel is centered at y_n , with bandwidth controlled by m . The corresponding probability mass function becomes

$$k_n(y \mid y_n, m) = \min \left\{ 1, \frac{p_n(y)}{p_n(y_n)} \right\} k_*(y \mid y_n, m) + \mathbb{1}(y = y_n) \left[1 - \frac{1}{2m + 1} \sum_{z=y_n-m}^{y_n+m} \min \left\{ 1, \frac{p_n(z)}{p_n(y_n)} \right\} \right],$$

for every $n \geq 1$, which has finite support $\{y_n - m, \dots, y_n + m\}$. When $m = 0$, the DP predictive distribution is recovered. Another simple possibility, paralleling classical choices in MCMC, is to choose a base kernel $k_*(y \mid y_n) = k_*(y)$ that does not depend on past observations, with $k_*(y)$ being a known distribution such as a Poisson or a negative binomial. This specification enforces a strong parametric structure and is suitable only when small deviations from a known model are expected. Although these two proposals lead to substantial computational simplifications, using more flexible kernels can improve predictive accuracy.

As an alternative, we recommend using a rounded Gaussian base kernel as in Canale and Dunson (2011), whose probability mass function is given by

$$k_*(y \mid y_n, \sigma) = \frac{\int_{y-1/2}^{y+1/2} \mathcal{N}(t \mid y_n, \sigma^2) dt}{\sum_{z \in \mathcal{Y}} \int_{z-1/2}^{z+1/2} \mathcal{N}(t \mid y_n, \sigma^2) dt},$$

for $n \geq 1$, where $\mathcal{N}(\cdot \mid y_n, \sigma^2)$ denotes a normal density function with mean y_n and variance σ^2 . Although σ controls the bandwidth of the rounded Gaussian base kernel k_* , this role changes slightly after the Metropolis adjustment, as illustrated in Figure 1. When $\sigma \rightarrow 0$, the MH kernel collapses to a point mass at y_n , recovering the DP update $k_n(y \mid y_n, \sigma) = \mathbb{1}(y = y_n)$. A similar behavior occurs as $\sigma \rightarrow \infty$, when the base kernel becomes very diffuse: for values of y such that $p_{n-1}(y)$ is close to zero $\gamma_n(y, y_n) \rightarrow 0$ and consequently the probability mass on y_n , $1 - \sum_{z \in \mathcal{Y}} \gamma_n(z, y_n) k_*(z \mid y_n, \sigma)$, increases, recovering again the DP update. For intermediate values of σ , the MH kernel is smoother, with $k_n(y \mid y_n, \sigma) = k_*(y \mid y_n, \sigma)$ when $\gamma_n(y, y_n) = 1$ for all $y \in \mathcal{Y}$. The bandwidth σ also impacts the posterior variability. The left panel of Figure 2 illustrates how σ influences the variance of $P_{n+1} \mid y_{1:n}$. For $\sigma = 0$, the DP is recovered, and the variance is maximum. In this case, (9) is proportional to the posterior variance induced by the DP. As σ grows, the kernel becomes more diffuse and the variance

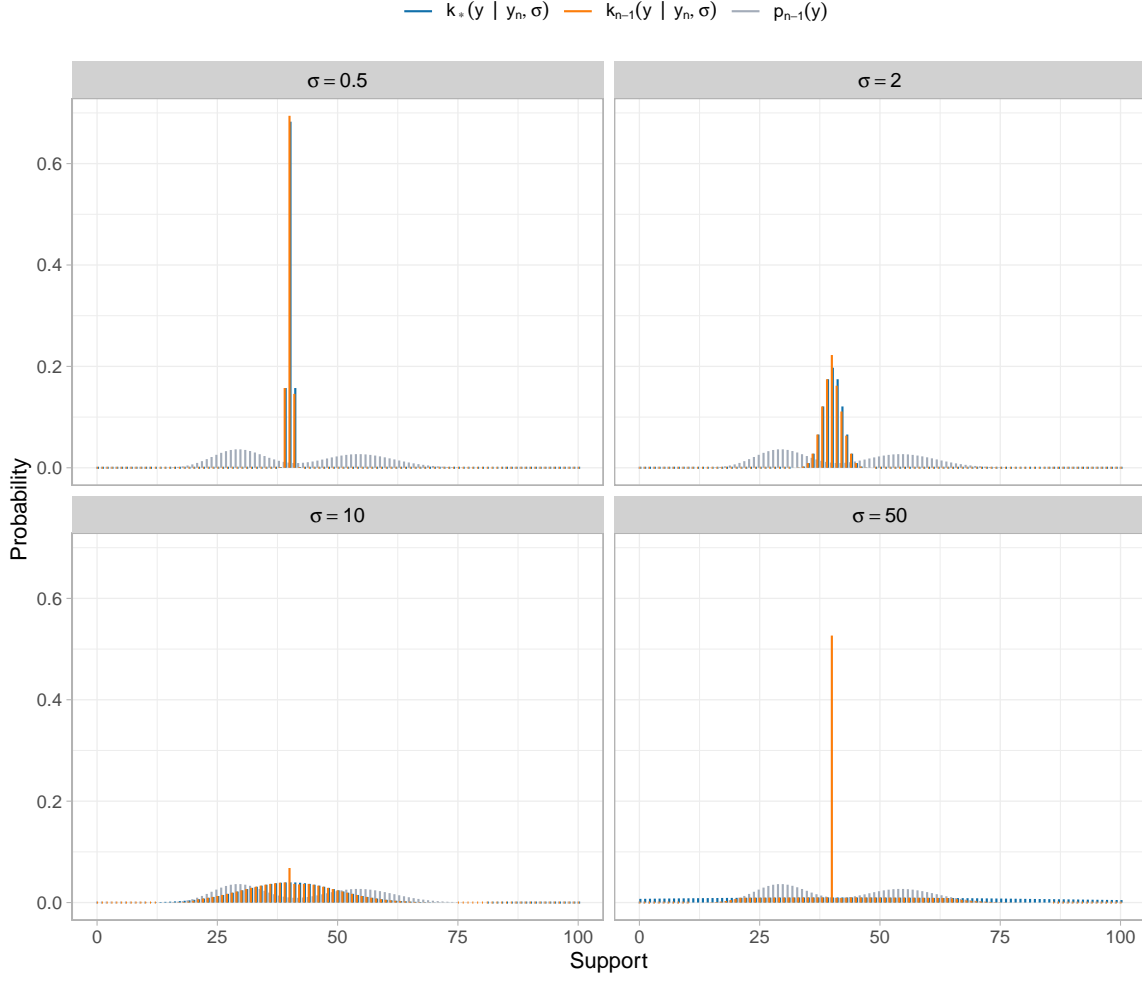


Figure 1: Example of the probability mass function of a MH kernel using a rounded Gaussian base kernel with $\sigma \in \{0.5, 2, 10, 50\}$ after observing $y_n = 40$.

dramatically decreases. The variance increases again for large values of σ , corresponding to concentrated MH kernels as discussed above. The bandwidth also has important consequences on the correlation. Unlike in the DP case, the induced correlation between any pair of disjoint sets A_1, A_2 for MAD sequences is not restricted to be negative, as illustrated in the right panel of Figure 2. This is a very appealing feature, because positive correlation enables borrowing of information between nearby values.

2.3 UNCERTAINTY QUANTIFICATION VIA PREDICTIVE RESAMPLING

A predictive resampling algorithm (Fortini and Petrone, 2020; Fong et al., 2023), described in Algorithm 1, can be used for approximate posterior sampling of P , whose law, unfortunately, is generally not available in closed form. Algorithm 1 can also be used for prior sampling of P by setting $n = 0$. Starting from P_n , the algorithm performs forward simulations by recursively sampling and updating the MAD predictive distribution. Each forward simulation generates a random dataset (Y_{n+1}, \dots, Y_N) which can

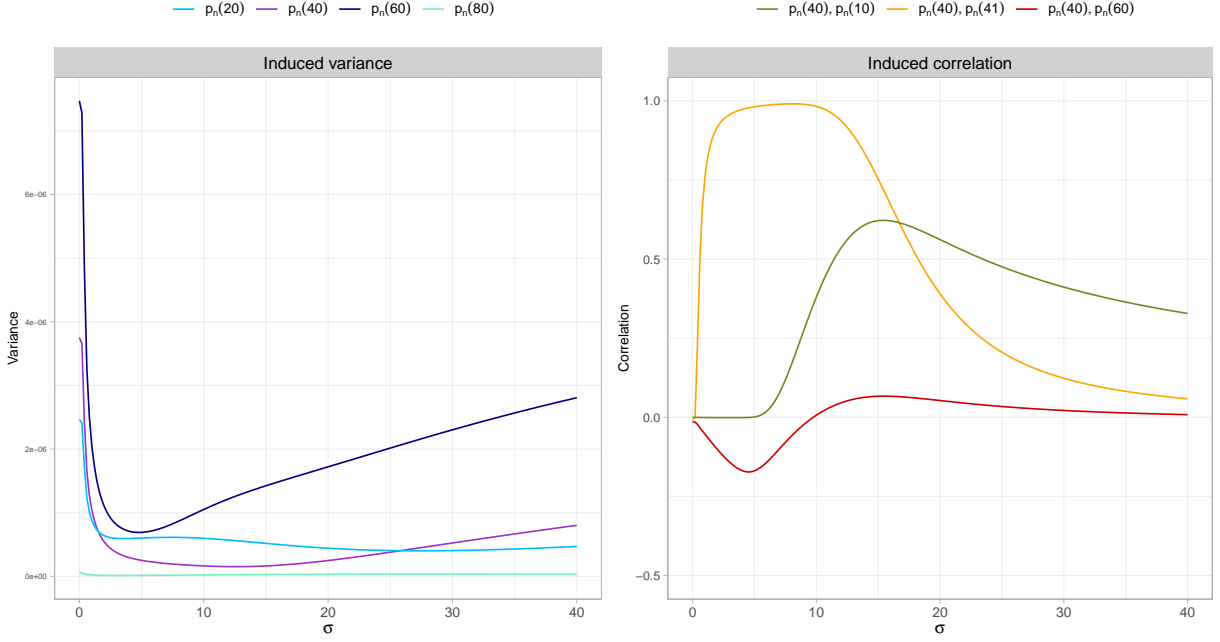


Figure 2: Left: posterior variance of $p_n(z)$ given $y_{1:n-1}$, with $z \in \{20, 40, 60, 80\}$. Right: correlation between $p_n(40)$ and $p_n(x)$ given $y_{1:n-1}$, with $x \in \{10, 41, 60\}$. For both panels, P_{n-1} is the same as in Figure 1.

be used to compute $P_N(\cdot)$ or any other statistic of interest, such as the population mean. By part (b) of Corollary 1, we can regard P_N as a finite-sample approximation of the limit distribution P for sufficiently large N . Consequently, the output of Algorithm 1 provides an approximate sample from the distribution of $P(\cdot) \mid y_{1:n}$.

Clearly, it is also possible to perform posterior inference on any functional $\theta = P(f)$. For example, if one is interested in the population mean $\theta = P(f) = \sum_{y \in \mathcal{Y}} y p(y)$, then the corresponding martingale posterior distribution can be approximated by considering its finite-sample version $\theta_N = P_N(f) = \sum_{y \in \mathcal{Y}} y p_N(y)$ which can be easily simulated using Algorithm 1. However, as previously mentioned, the posterior mean does not require approximations nor sampling, as we have $\mathbb{E}(\theta \mid y_{1:n}) = \theta_n$ thanks to the martingale property.

Remark 2. The discreteness of the MAD predictive rule is computationally advantageous compared to the continuous case (e.g. Fong et al., 2023). First, despite what the Metropolis–Hastings terminology might suggest, the recursive update of p_n does not involve any sampling, as p_n can be directly updated using the definition of the kernel $k_n(y \mid y_n)$. This update is straightforward when both p_0 and the base kernel k_* have finite support, since p_n can then be represented by a finite set of probability weights. Sampling from p_n is also straightforward, again because it involves a finite set of probabilities. In the countable case, it suffices to truncate p_n by removing support points with negligible probability, which is effectively equivalent to using a base kernel with finite support.

Algorithm 1 Predictive resampling (Fortini and Petrone, 2020; Fong et al., 2023)

Compute p_n as in (3) from the observed data $y_{1:n}$

Set $N \gg n$

for $j = 1, \dots, B$ **do**

for $i = n + 1, \dots, N$ **do**

 Sample $Y_i \mid y_{1:i-1} \sim p_{i-1}$

 Update $p_i(y) = (1 - w_i)p_{i-1}(y) + w_i k_i(y \mid y_i)$

end for

end for

return $p_N^{(1)}(y), \dots, p_N^{(B)}(y)$, an iid sample of size B from the distribution of $p_N(\cdot) \mid y_{1:n}$

2.4 ASYMPTOTIC BEHAVIOUR

In this section, we establish a predictive central limit theorem for MAD sequences. Specifically, for any $H \geq 1$ and any measurable sets A_1, \dots, A_H , we derive a Gaussian approximation for the posterior distribution of $P(A_1), \dots, P(A_H) \mid y_{1:n}$ as $n \rightarrow \infty$. Intuitively, our result quantifies the uncertainty that arises from observing a finite sample of size n instead of the infinite population. Within the Bayesian predictive literature, Fortini and Petrone (2020) provide a predictive central limit theorem for the Newton estimator, while Fong and Yiu (2024a) obtain a similar result for parametric martingale posteriors. The following results specialize those of Fortini and Petrone (2025) for general CID sequences; however, in the context of MAD sequences, some of their assumptions are not required, and therefore the proof is provided. Consistent with Fortini and Petrone (2020, 2025) and Fong and Yiu (2024a), the proof relies on a martingale central limit theorem formulated in terms of almost sure conditional convergence (Crimaldi, 2009), a notion of convergence that implies stable convergence (Rényi, 1963; Häusler and Luschgy, 2015). Stable convergence, which is stronger than convergence in distribution but weaker than convergence in probability, plays a central role in martingale central limit theorems, especially when the limiting variance is random.

Proposition 1. *Let $(Y_n)_{n \geq 1}$ be a MAD sequence and let $(r_n)_{n \geq 1}$ be a monotone sequence of positive numbers such that $r_n \doteq (\sum_{k > n} w_k^2)^{-1}$ as $n \rightarrow \infty$. Assume $\sqrt{r_n} \sup_{k \geq n} w_k \rightarrow 0$, $\sum_{k \geq 1} r_k^2 w_{k+1}^4 < \infty$, and that, for every $H \geq 1$ and all measurable sets A_1, \dots, A_H , the random matrix $\Sigma = \Sigma(A_1, \dots, A_H) = [\Sigma_{jt}]$, $j, t = 1, \dots, H$, with*

$$\Sigma_{jt} = \sum_{y \in \mathcal{Y}} K(A_j \mid y) K(A_t \mid y) p(y) - P(A_j) P(A_t), \quad (11)$$

where $K(A \mid y) = \sum_{x \in A} k(x \mid y)$ and

$$k(x \mid y) = \gamma(x, y) k_*(x \mid y) + \mathbf{1}(x = y) \left[1 - \sum_{z \in \mathcal{Y}} \gamma(z, y) k_*(z, y) \right], \quad \gamma(x, y) = \min \left\{ 1, \frac{p(x) k_*(y \mid x)}{p(y) k_*(x \mid y)} \right\},$$

is positive definite. Then, for every $H \geq 1$ and every A_1, \dots, A_H ,

$$\sqrt{r_n} \begin{bmatrix} P(A_1) - P_n(A_1) \\ \dots \\ P(A_H) - P_n(A_H) \end{bmatrix} \Big| Y_{1:n} \xrightarrow{d} \mathbf{Z}, \quad \mathbf{Z} \sim \mathcal{N}_H(\mathbf{0}, \mathbf{\Sigma}),$$

\mathbb{P} -a.s. for $n \rightarrow \infty$, where $\mathcal{N}_H(\mathbf{0}, \mathbf{\Sigma})$ denotes a H -dimensional Gaussian distribution with mean $\mathbf{0}$ and covariance $\mathbf{\Sigma}$.

The proposition shows that the posterior distribution of P concentrates around its expectation P_n at a convergence rate of $1/\sqrt{r_n}$. The asymptotic variance $\mathbf{\Sigma}$ is random, as it depends on the entire sequence (Y_1, Y_2, \dots) . Having a random limit for the covariance is common in martingale central limit theorems and Bayesian predictive inference (see Fortini and Petrone, 2020, 2025; Berti et al., 2021; Fong and Yiu, 2024a). This result should not be regarded as a Bernstein–von Mises asymptotic Gaussian approximation for the posterior distribution, because Proposition 1 is formulated under the joint law \mathbb{P} and does not assume the Y_i are iid from a true underlying distribution.

Proposition 1 provides insight into the prior variance induced by MAD sequences: if $n = 0$ then $\mathbf{\Sigma}$ corresponds to the implicit prior variance, which depends on the limit distribution P . For $n \geq 1$, the interpretation is less straightforward, as the asymptotic variance now depends on both past and future observations. However, each element of the random covariance in (11) is proportional to the \mathbb{P} -a.s. limit of the previously considered finite-sample covariance

$$\text{cov}\{P_{n+1}(A_j), P_{n+1}(A_t) \mid y_{1:n}\} = w_{n+1}^2 \sum_{y \in \mathcal{Y}} K_n(A_j \mid y) K_n(A_t \mid y) p_n(y) - P_n(A_j) P_n(A_t), \quad (12)$$

for any $j, t = 1, \dots, H$. Consequently, we can employ (12) to approximate $\mathbf{\Sigma}$.

Proposition 2. For every $n \geq 1$ and all measurable sets A_1, \dots, A_H , let $\mathbf{\Sigma}_n = \mathbf{\Sigma}_n(A_1, \dots, A_H) = [\Sigma_{n,jt}]$, $j, t = 1, \dots, H$, with

$$\Sigma_{n,jt} = \sum_{y \in \mathcal{Y}} K_n(A_j \mid y) K_n(A_t \mid y) p_n(y) - P_n(A_j) P_n(A_t).$$

Then, under the assumptions of Proposition 1, \mathbb{P} -a.s., $\mathbf{\Sigma}_n \rightarrow \mathbf{\Sigma}$ and

$$\sqrt{r_n} \mathbf{\Sigma}_n^{-1/2} \begin{bmatrix} P(A_1) - P_n(A_1) \\ \dots \\ P(A_H) - P_n(A_H) \end{bmatrix} \Big| y_{1:n} \xrightarrow{d} \mathbf{Z}, \quad \mathbf{Z} \sim \mathcal{N}_H(\mathbf{0}, \mathbf{I}),$$

for $n \rightarrow \infty$, where \mathbf{I} denotes the identity matrix.

Remark 3. The results of Propositions 1 and 2 hold when $w_n = (\alpha + n)^{-\lambda}$ with $r_n = (2\lambda - 1)n^{2\lambda-1}$.

Replacement of the random matrix Σ with its estimate Σ_n is possible due to stable convergence. Proposition 2 highlights the relationship between the posterior variance and one-step-ahead predictive updates. This connection becomes particularly evident in the case $H = 1$, where, for large n , the distribution of $P(A) \mid y_{1:n}$ can be approximated by $\mathcal{N}(P_n(A), \Sigma_n r_n^{-1})$, with $\Sigma_n = \sum_{y \in \mathcal{Y}} K_n(A \mid y)^2 p_n(y) - P_n(A)^2$. Therefore, as noted also by Fortini and Petrone (2020, 2025) and Fong and Yiu (2024a), the asymptotic posterior variance of $P(A)$ is connected to the expected squared predictive update from $P_n(A)$ to $P_{n+1}(A)$ given $y_{1:n}$ with

$$\Sigma_n r_n^{-1} \approx \Sigma_n \sum_{k>n} w_k^2 = \mathbb{E}\{[P_{n+1}(A) - P_n(A)]^2 \mid y_{1:n}\} \sum_{k>n+1} w_k^2 \quad (13)$$

for n large. Equation (13) provides insights on the relationship between the learning rate of the predictive rule and the posterior variability, highlighting the crucial role played by the weights w_n : while weights that decay to zero quickly induce fast learning and convergence to the asymptotic exchangeability regime, small values of w_n may result in poor learning and underestimation of the posterior variability.

Although the standard choice for the DP is $w_n = (\alpha + n)^{-1}$, it has been observed that such weights may decay to zero too quickly according to frequentist criteria, making them unappealing for CID modelling (see Fortini and Petrone, 2020; Fong et al., 2023). To address this, the literature has proposed alternatives with slower decay rates, such as $w_n = (\alpha + n)^{-2/3}$ (Martin and Tokdar, 2009), and $w_n = (2 - n^{-1})(n + 1)^{-1}$ (Fong et al., 2023). Alternatively, Fortini and Petrone (2020) suggest using adaptive weights of the form $w_n = (\alpha + n)^{-\lambda_n}$, where $\lambda_n = 1$ for $n \leq N_*$ to allow fast convergence, and $\lambda_n = 3/4$ when $n > N_*$ induces slower decay once an approximate exchangeability regime is reached. Although this split-sample approach is appealing, a smoother transition between the two regimes is desirable. For this reason, we consider the adaptive weights with

$$\lambda_n = \lambda + (1 - \lambda) \exp \left\{ -\frac{1}{N_*} n \right\}, \quad (14)$$

with $\lambda \in (1/2, 1]$ and $N_* > 0$. Using (14), the weights behave as $w_n \approx (\alpha + n)^{-1}$ for small n , smoothly transitioning to $w_n \approx (\alpha + n)^{-\lambda}$ as n increases. The transition rate is governed by N_* , which should be chosen such that the sequence is approximately in an exchangeable regime beyond that point. A practical default is to set $N_* = N/2$, where N denotes the length of each forward simulation in the predictive resampling algorithm. Following Fortini and Petrone (2020), we adopt $\lambda = 3/4$ in our analyses. The implications of these different weighting options for the MAD sequences are explored in Section 4.

2.5 UNIVARIATE ILLUSTRATIVE EXAMPLE

We provide a simulated example to illustrate the MAD sequence and compare it with the DP. We generate $n = 50$ data points from the mixture $0.4 \text{Poisson}(y; 25) + 0.6 \text{Poisson}(y; 60)$. We consider two

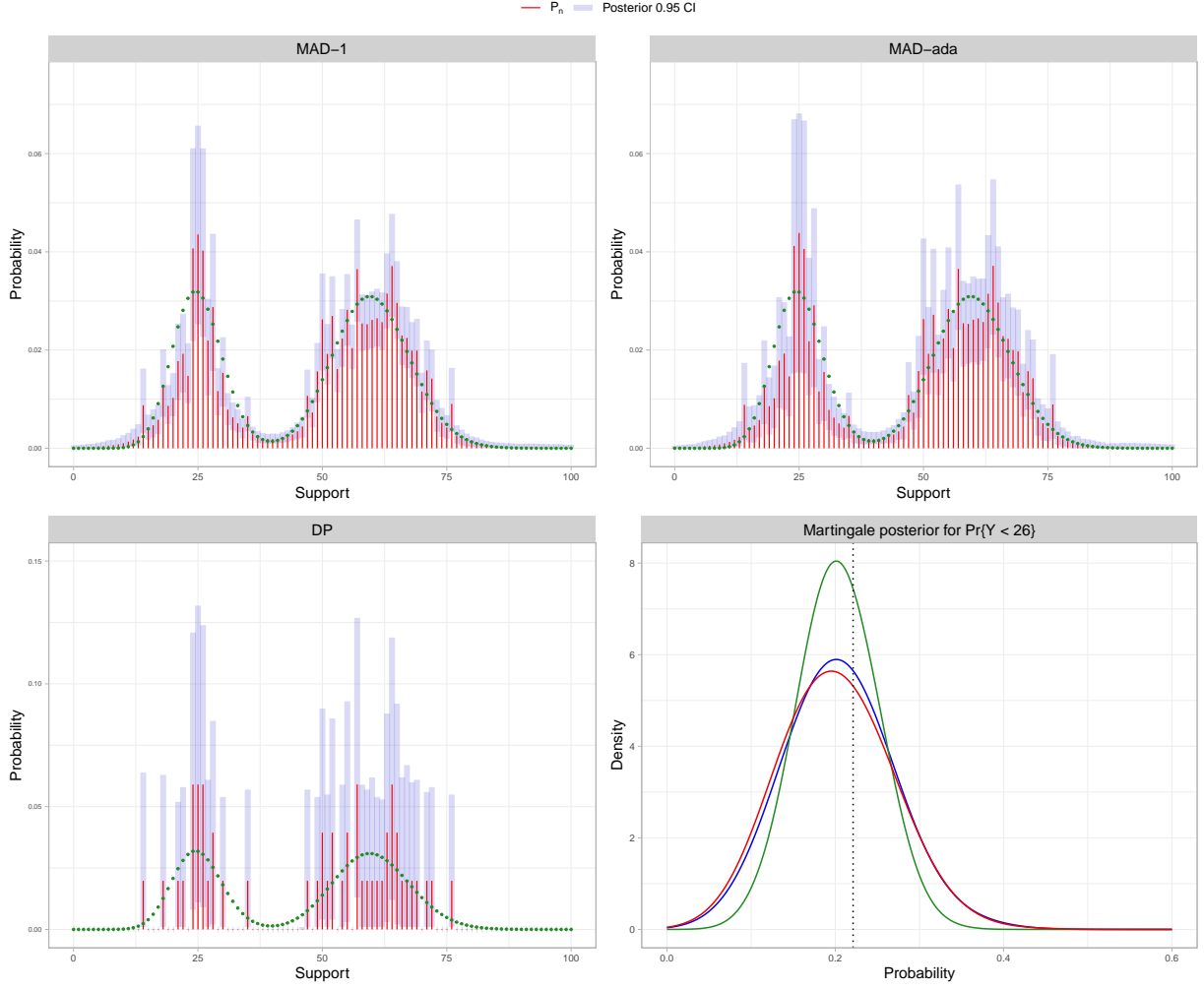


Figure 3: Predictive distributions obtained using a MAD sequence with $w_n = (\alpha + n)^{-1}$ (MAD-1), with adaptive weights $w_n = (\alpha + n)^{-\lambda_n}$ (MAD-ada), and with the DP. The dotted line represents the probability mass function of the true data generator. The bottom-right panel shows the martingale posterior distribution for the probability that $Y \leq 25$ using MAD-1 (green), MAD-ada (red) and DP (blue), with the dotted line representing the true value.

variants of MAD sequences, having $w_n = (\alpha + n)^{-1}$ and $w_n = (\alpha + n)^{-\lambda_n}$, with λ_n defined in (14), $\lambda = 3/4$ and $N_* = 500$. For updating the MAD sequences, we choose a uniform base measure P_0 over the support, which we restrict to $\{0, \dots, 100\}$, and set $\alpha = 1$. We employ rounded Gaussian base kernels, and we recommend selecting σ using a data-driven approach. Following Fong et al. (2023), we rely on the notion of prequential log-likelihood introduced by Dawid (1984). Specifically, under the predictive construction (4), the quantity $\sum_{i=1}^n \log p_{i-1}(y_i)$ can be interpreted as a log-likelihood function, making its maximization a natural criterion for selecting σ . Alternatively, one can tune σ using the methods available for KDE, such as minimizing the prediction error in a validation set or by cross-validation.

Uncertainty quantification is carried out by predictive resampling $N = 1000$ future observations starting from P_n and obtaining $B = 1000$ samples from the corresponding martingale posterior. By

replacing exchangeability with the CID condition, MAD predictive distributions depend on the ordering of $y_{1:n}$. To ensure permutation invariance, we compute P_n averaging over S permutations of the data. Consistently with Fong et al. (2023), we found that $S = 10$ is sufficient in practice. Computations for different permutations can be performed in parallel. The prequential log-likelihood for selecting the optimal σ is also averaged over the S permutations, whereas the predictive resampling algorithm starts from the permutation averaged P_n .

Figure 3 shows the predictive distributions obtained using the two variants of MAD sequences and DP. Both weight options provide similar MAD predictive distributions and the improvement over the DP is substantial. The MAD sequences effectively capture the two components of the mixture, assigning lower probabilities in the tails and in the region between the modes. Moreover, as empirically shown in Appendix C, MAD sequences converge to the true distribution faster than the DP. For each value $y \in \mathcal{Y}$, Figure 3 also includes the 95% credible interval for $p_N(y)$. Additionally, the bottom-left panel of Figure 3 presents the martingale posterior distribution for the quantity $\theta_N = P_N((-\infty, 25]) = \sum_{y \in \mathcal{Y}} \mathbb{1}(y \leq 25)p_N(y)$, computed as described in Section 2.3. As discussed in Section 2.4, the adaptive weights yield a more conservative uncertainty quantification compared to the standard choice $w_n = (\alpha + n)^{-1}$. This results in wider 95% credible intervals for $P_N(y)$ and a less concentrated martingale posterior for θ .

3 MULTIVARIATE MODELING

In this section, we consider MAD sequences for modeling multivariate count data. Let $\mathbf{y}_n = (y_{n1}, \dots, y_{nd}) \in \mathcal{Y} = \{0, 1, \dots\}^d$ be a realization of the random vector $\mathbf{Y}_n = (Y_{n1}, \dots, Y_{nd})$, for $n \geq 1$ and $d \geq 2$, and denote $\mathbf{y}_{1:n} = (\mathbf{y}_1^\top, \dots, \mathbf{y}_n^\top)$. Assuming the sequential generating mechanism (4) for $(\mathbf{Y}_n)_{n \geq 1}$, the multivariate MAD predictive distribution has probability mass function

$$p_n(\mathbf{y}) = \mathbb{P}(Y_{n+1,1} = y_1, \dots, Y_{n+1,d} = y_d \mid \mathbf{y}_{1:n}) = (1 - w_n)p_{n-1}(\mathbf{y}) + w_n k_n(\mathbf{y} \mid \mathbf{y}_n),$$

where the multivariate MH kernel retains the same structure as in the univariate case, since the corresponding probability mass function is

$$k_n(\mathbf{y} \mid \mathbf{y}_n) = \gamma_n(\mathbf{y}, \mathbf{y}_n) k_*(\mathbf{y} \mid \mathbf{y}_n) + \mathbb{1}(\mathbf{y} = \mathbf{y}_n) \left[\sum_{\mathbf{z} \in \mathcal{Y}} \left\{ 1 - \gamma_n(\mathbf{z}, \mathbf{y}_n) \right\} k_*(\mathbf{z}, \mathbf{y}_n) \right],$$

with

$$\gamma_n(\mathbf{y}, \mathbf{y}_n) = \min \left\{ 1, \frac{p_{n-1}(\mathbf{y}) k_*(\mathbf{y}_n \mid \mathbf{y})}{p_{n-1}(\mathbf{y}_n) k_*(\mathbf{y} \mid \mathbf{y}_n)} \right\}.$$

The above equations can be formally regarded as special cases of the general definition in (3), (5), and (6), but the multivariate nature of the data is emphasized using the bold notation. Any discrete multivariate distribution can be chosen as base kernel. A simple and reasonable choice is a factorized

base kernel having rounded Gaussian distribution components,

$$k_*(\mathbf{y} \mid \mathbf{y}_n, \boldsymbol{\sigma}) = \prod_{j=1}^d k_*(y_j \mid y_{nj}, \sigma_j),$$

with $\boldsymbol{\sigma} = (\sigma_1, \dots, \sigma_d)$. This factorized structure again parallels common practice in standard multivariate KDE. More complex kernels that induce dependence between components can also be adopted.

Remark 4. MAD sequences are defined on a general countable space \mathcal{Y} , which includes $\mathcal{Y} = \{0, 1, \dots\}^d$ as a special case. Hence, the results of Theorem 1 and Corollary 1, as well as those of Propositions 1–2, hold for multivariate MAD sequences. The multivariate case requires special attention, as the choice of the base kernel is less straightforward, and the practical implications deserve careful discussion.

There are several advantages of multivariate MAD sequences compared to existing approaches. First, although DP mixtures of multivariate rounded Gaussian kernels with non-diagonal covariance matrices (Canale and Dunson, 2011) can be used to model multivariate count probability mass functions, MCMC computation can be inefficient. Conceptually, the predictive mixture model of Fortini and Petrone (2020) can address this issue, but in practice, the associated Newton algorithm requires the numerical evaluation of a multidimensional integral at each iteration. In contrast, employing MH kernels makes the extension to multivariate MAD sequences both straightforward and computationally tractable, as only univariate Gaussian integrals are involved, for which efficient numerical methods are available. Furthermore, unlike the multivariate method proposed by Fong et al. (2023), which depends on the order in which dimensions are updated, multivariate MAD sequences are invariant to the dimension ordering. For the copula update, the CID assumption holds only under a fixed ordering of the variables, and different orderings lead to distinct predictive distributions. This sensitivity is unappealing in practice. In contrast, MAD sequences assume that $(\mathbf{Y}_n)_{n \geq 1}$ is a CID sequence regardless of the variable ordering. In Appendix B, we examine the dimension-ordering dependence of the copula update in a simulation study and compare the results with those obtained from MAD sequences.

3.1 MULTIVARIATE BINARY DATA

Multivariate MAD sequences can also be adapted to model multivariate binary data. Due to the flexibility of MH kernels, this extension is straightforward, requiring only the selection of an appropriate base kernel. For $\mathbf{y} \in \{0, 1\}^d$, we propose to employ the base kernel that has probability mass function

$$k_*(\mathbf{y} \mid \mathbf{y}_n) = \prod_{j=1}^d k_*(y_j \mid y_{nj}),$$

where

$$k_*(y_j \mid y_{nj}) = |y_{nj} - \delta|^{y_j} (1 - |y_{nj} - \delta|)^{(1-y_j)} = \begin{cases} \delta^{y_j} (1 - \delta)^{1-y_j} & \text{if } y_{nj} = 0 \\ (1 - \delta)^{y_j} \delta^{1-y_j} & \text{if } y_{nj} = 1 \end{cases} \quad (15)$$

for $j = 1, \dots, d$ and $\delta \in [0, 0.5]$. An example of (15) for different values of δ is shown in Appendix C. Roughly speaking, for each dimension j , if $y_{nj} = 1$ the base kernel assigns probability $(1 - \delta) \geq 0.5$ to the event $Y_{n+1,j} = 1$ and non-zero probability $\delta \leq 0.5$ to the event $Y_{n+1,j} = 0$, and vice versa. For $\delta = 0$, the DP update is recovered, while for $\delta = 0.5$, a uniform base kernel is obtained. A practical default is to set $\delta = 0.25$, or δ can be estimated using the prequential log-likelihood technique in Section 2.2.

3.2 NONPARAMETRIC REGRESSION AND CLASSIFICATION

An important consequence of the multivariate approach is the possibility of using MAD sequences for nonparametric regression and classification. Let each covariate vector $\mathbf{x}_n \in \mathcal{X} \subseteq \{0, 1, \dots\}^d$ be a realization of the random vector \mathbf{X}_n . Then, we can first estimate the joint probability mass function $p_n(y, \mathbf{x})$ based on the joint CID sequence $(Y_1, \mathbf{X}_1), \dots, (Y_n, \mathbf{X}_n)$, and then compute the conditional predictive distribution $p_n(y | \mathbf{x})$, with $p_n(y | \mathbf{x}) = p_n(y, \mathbf{x}) / p_n(\mathbf{x})$. In this case, predictive resampling requires jointly sampling $(Y_{n+1}, \mathbf{X}_{n+1}) \sim p_n(y, \mathbf{x})$. The response variable Y_n can also be multivariate, possibly including both binary and count-valued components. Moreover, the framework can incorporate continuous covariates by combining discrete MH kernels with the bivariate Gaussian copula update proposed by Fong et al. (2023). We provide simulation examples of count data regression and classification with binary covariates in Section 4.

4 SIMULATION STUDIES

In this section, we present two simulation studies comparing MAD sequences with established machine learning methods for count data regression and classification. The studies assess both the predictive accuracy and the quality of uncertainty quantification. A separate simulation comparing MAD sequences with the copula updating approach of Fong et al. (2023) is provided in Appendix B.

4.1 COUNT DATA REGRESSION WITH BINARY COVARIATES

Nonparametric methods are especially useful for capturing nonlinear relationships between variables. To demonstrate the effectiveness of MAD sequences in nonlinear regression settings, we conducted a simulation study comparing our approach with well-established machine learning methods, such as random forests and Bayesian additive regression trees (BART; Chipman et al., 2010). Although machine learning methods typically excel with large sample sizes, we expect that MAD sequences offer better performance in small-sample scenarios. As additional benchmarks, we include the DP and the Poisson generalized linear model (GLM). For each sample size $n \in \{40, 80\}$, we generate 50 simulated datasets. For each simulation, we include 10 binary covariates sampled from independent binomial distributions

with parameter 0.5, and $Y_i \mid \mathbf{x}_i \sim \text{Poi}(e^{\eta_i})$, where

$$\eta_i = 1 + \sqrt{|-0.5x_{i,1} + 1.5x_{i,2} + x_{i,3} + 0.5x_{i,4} - 0.5x_{i,5}|} + (-0.7x_{i,6} + 0.5x_{i,7} + 0.7x_{i,8} - 0.3x_{i,9} - 0.3x_{i,10})^2.$$

The study assesses the performance of each method by comparing the accuracy of out-of-sample predictions and uncertainty quantification. For predictive accuracy, we compute the mean squared error (MSE) obtained on 10^4 new observations. To evaluate uncertainty quantification accuracy, we consider the frequentist coverage of the 95% credible intervals for $\mathbb{E}(Y \mid \mathbf{x})$, calculated across 50 simulations for each of the $2^{10} = 1024$ possible values for the covariate vector \mathbf{x} . For random forests, we consider the predictive confidence intervals proposed by [Mentch and Hooker \(2016\)](#).

Since the posterior variability of MAD sequences depends on the choice of the weights w_n , we compare four variants of MAD sequences using the options discussed in Section 2.4: $w_n = (\alpha + n)^{-1}$ (MAD-1), $w_n = (\alpha + n)^{-2/3}$ (MAD-2/3), the weights $w_n = (2 - n^{-1})(n + 1)^{-1}$ proposed by [Fong et al. \(2023\)](#) (MAD-DPM), and the adaptive solution $w_n = (\alpha + n)^{\lambda_n}$, with λ_n defined in Equation (14) (MAD-ADA). We use a weakly informative uniform base measure over the support and set $\alpha = 1$. For the adaptive weights, we set $\lambda = 3/4$ and $N_* = 500$. Each MAD sequence employs a rounded Gaussian base kernel for the response, with bandwidth selected by maximizing the prequential log-likelihood. The hyperparameters for the binary base kernels for the covariates are set to the default value 0.25. To ensure permutation invariance, we average the predictive distribution and the prequential log-likelihood over 10 random permutations of the data. To compute the martingale posterior distributions we draw $B = 200$ samples from P_N using a predictive resampling algorithm with $N = n + 1000$. For point prediction with MAD sequences, we use the population mean $\theta_n = \sum_{y \in \mathcal{Y}} y p_n(y \mid \mathbf{x})$, while for uncertainty quantification, we employ the credible intervals obtained from the martingale posterior for the population mean, as described in Section 2.3.

The MSE and coverage results obtained across the 50 simulated datasets are reported in Table 1. Since it does not allow the borrowing of information between nearby locations, the DP overfits the observed data, consequently leading to poor out-of-sample point predictions and inaccurate credible intervals. In terms of predictive accuracy, as expected, MAD sequences perform substantially better than the Poisson GLM, which fails to capture nonlinear effects. The four variants of MAD sequences exhibit similar predictive performance, indicating that the choice of weights has little impact on the point estimate. Furthermore, all MAD sequences provide a better prediction accuracy than random forest and BART for both $n = 40$ and $n = 80$.

In terms of uncertainty quantification, the credible intervals produced by the MAD sequence with adaptive weights are, on average, well calibrated for both sample sizes considered. In contrast, alternative weighting strategies tend to result in undercoverage. However, we observe substantial variability in empirical coverage in $2^{10} = 1024$ possible covariate configurations. Although the Poisson GLM and BART models exhibit less variability in coverage across covariate settings, they consistently fall below

Table 1: Out-of-sample MSE evaluated on 10^4 new observations and median frequentist coverage for the 95% credible intervals for $\mathbb{E}(Y \mid \mathbf{x})$ for each of the 1024 possible values of the covariate vector \mathbf{x} . The results are obtained by averaging 50 simulated datasets. Bold values represent the lowest MSE among the proposed methods and the lowest MSE among the competitors, for each scenario. Standard error and interquartile range are reported in brackets for MSE and median coverage, respectively.

Regression	$n = 40$				$n = 80$			
	MSE		Median coverage		MSE		Median coverage	
GLM	120.77	[51.51]	0.84	[0.70, 0.90]	94.93	[8.37]	0.90	[0.74, 0.96]
BART	101.17	[12.69]	0.92	[0.82, 0.96]	74.17	[10.00]	0.92	[0.84, 0.96]
RF	99.98	[7.45]	1.00	[0.92, 1.00]	87.75	[6.53]	1.00	[1.00, 1.00]
DP	1450.21	[5.53]	0.00	[0.00, 0.00]	1395.61	[8.72]	0.00	[0.00, 0.00]
MAD-1	91.07	[10.35]	0.92	[0.68, 0.98]	73.96	[7.60]	0.88	[0.58, 0.98]
MAD-2/3	88.83	[13.00]	0.92	[0.50, 0.98]	73.18	[9.58]	0.94	[0.56, 1.00]
MAD-DPM	87.41	[12.36]	0.90	[0.52, 0.98]	72.07	[9.48]	0.92	[0.54, 1.00]
MAD-ADA	90.61	[10.28]	0.96	[0.77, 1.00]	73.45	[7.69]	0.96	[0.64, 1.00]

the nominal level, indicating systematic undercoverage. Random forests produce overly conservative credible intervals, with coverage levels substantially exceeding 0.95.

4.2 CLASSIFICATION WITH BINARY COVARIATES

We also conducted a simulation study focused on binary classification from 10 binary covariates. We generated 50 simulated datasets for each sample size $n = \{150, 300\}$. We sample $y_i \mid \mathbf{x}_i$ from $\text{Bin}\{1, \text{logit}^{-1}(\eta_i)\}$, with

$$\eta_i = -3 + 2x_{i,1} - 4x_{i,2} + 3x_{i,3} - 3x_{i,4} - 3x_{i,5}x_{i,6} + \sqrt{|2x_{i,7} - 3x_{i,8}|} + (3x_{i,9} - 2x_{i,10})^2,$$

$i = 1, \dots, n$, and draw $x_{i,j} \sim \text{Bernoulli}(\tau_j)$, $j = 1, \dots, 10$, with $\boldsymbol{\tau} = (0.45, 0.65, 0.7, 0.4, 0.4, 0.6, 0.7, 0.3, 0.55, 0.55)$ independently. We considered the variants of MAD sequences described in Section 4.1 for count data regression. The hyperparameters for the binary base kernels for the covariates are set to the default value of 0.25, while the response hyperparameter is selected by maximizing the prequential log-likelihood. We compare with DP, logistic GLM, BART, and random forest. We evaluated out-of-sample predictive accuracy using the ROC curve computed on 10^4 new observations, and compared the corresponding area under the curve (AUC). Uncertainty quantification performance is evaluated as in Section 4.1. The results are reported in Table 2.

In terms of predictive accuracy, MAD sequences outperform both the DP and logistic GLM models, and are competitive with BART and random forests, particularly when $n = 150$. For $n = 300$, BART and random forests produce slightly more accurate point predictions; however, the credible intervals

Table 2: Out-of-sample AUC evaluated on 10^4 new observations and median frequentist coverage for the 95% credible intervals for $\mathbb{E}(Y \mid \mathbf{x})$ for each of the 1024 possible values of the covariate vector \mathbf{x} . The results are obtained by averaging 50 simulated datasets. Bold values represent the highest AUC among the proposed methods and the highest AUC among the competitors, for each scenario. Standard error and interquartile range are reported in brackets for AUC and median coverage, respectively.

Classification	$n = 150$				$n = 300$			
	AUC		Median coverage		AUC		Median coverage	
GLM	0.796	[0.014]	0.18	[0.06, 0.46]	0.809	[0.007]	0.00	[0.00, 0.20]
BART	0.863	[0.026]	0.18	[0.00, 0.71]	0.932	[0.009]	0.22	[0.00, 0.80]
RF	0.882	[0.025]	0.18	[0.10, 0.38]	0.913	[0.015]	0.70	[0.60, 0.84]
DP	0.644	[0.011]	0.00	[0.00, 0.00]	0.724	[0.012]	0.00	[0.00, 0.02]
MAD-1	0.873	[0.014]	0.44	[0.08, 0.73]	0.899	[0.008]	0.34	[0.02, 0.68]
MAD-2/3	0.869	[0.015]	0.86	[0.72, 0.96]	0.899	[0.009]	0.98	[0.92, 1.00]
MAD-DPM	0.872	[0.014]	0.72	[0.52, 0.89]	0.901	[0.008]	0.74	[0.48, 0.90]
MAD-ADA	0.874	[0.014]	0.82	[0.62, 0.94]	0.900	[0.008]	0.90	[0.72, 0.98]

produced by MAD sequences are significantly better calibrated in terms of frequentist coverage. In particular, although we do not claim optimal calibration guarantees, MAD sequences with weights $w_n = (\alpha + n)^{-2/3}$, as well as those using adaptive weights, produce 95% credible intervals with empirical coverage close to the nominal level, especially when $n = 300$. In contrast, while providing good point predictions, the standard choice $w_n = (\alpha + n)^{-1}$ results in poorly calibrated credible intervals.

5 APPLICATION: CORVIDS ABUNDANCE IN FINLAND

We analyze data from an ecological monitoring study of birds in Finland (Lindström et al., 2015), focusing on the occurrence rates of corvids in year 2009. Specifically, four species of the survey belong to the corvid family (*Corvidae*): carrion crow (*Corvus corone*), Eurasian magpie (*Pica pica*), common raven (*Corvus corax*), and Eurasian jay (*Garrulus glandarius*). Corvids are non-migratory birds that occur throughout Finland. Monitoring their abundance is particularly important, as they can respond to habitat and climate changes more rapidly than most other species (Jokimäki et al., 2022). Moreover, their presence influences ecological balance, given their efficiency as predators and their ability to live in close associations with humans (Madden et al., 2015). The study includes observations from $n = 76$ different sites. For each observation, the data set includes environmental covariates that include habitat type (broad leaf forest, coniferous forest, open habitat, urban habitat, or wetlands) and temperature in April-May (classified as cold, mild or warm if the registered average temperature is below 5°C , between 5° and 7.5°C , or above 7.5°C , respectively).

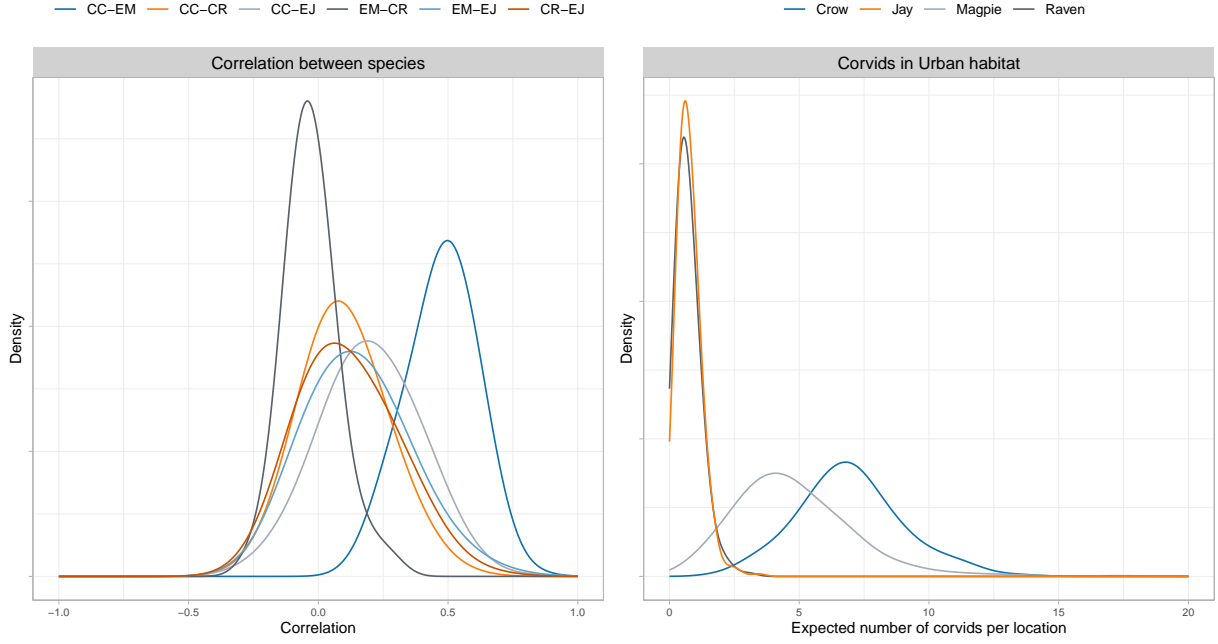


Figure 4: Left: posterior distribution for the correlation across species, with CC, EM, CR, and EJ denoting common crow, Eurasian magpie, common raven, and Eurasian jay, respectively. Right: posterior distribution of the expected number of corvids observed at each urban habitat location.

Modeling bird species abundance data presents several challenges: count data are often zero inflated and overdispersed relative to the Poisson distribution, and the dependence structure between species is unknown a priori. MAD sequences are particularly well suited for modeling such data, as their flexibility allows us to effectively address zero inflation and overdispersion while capturing across species dependence through the multivariate MH kernels described in Section 3. We compare MAD sequences with three widely used methods in ecological modeling: hierarchical modeling of species communities (HMSC; [Ovaskainen et al., 2016](#); [Tikhonov et al., 2017](#); [Ovaskainen and Abrego, 2020](#)), generalized joint attribute models (GJAMS; [Clark et al., 2017](#)), and generalized linear latent variable models (GLLVMS; [Skrondal and Rabe-Hesketh, 2004](#)). These models capture species dependence by incorporating latent variables in the linear predictor, and HMSC additionally includes site-specific random intercepts. To account for overdispersion and zero inflation, we consider negative binomial (GLLVM-NB) and zero-inflated negative binomial (GLLVM-ZINB) distributions for the response in GLLVMS.

For the MAD sequence, we choose the adaptive weights $w_n = (\alpha + n)^{-\lambda_n}$, with λ_n defined in Equation (14). We use a weakly informative uniform base measure setting $\alpha = 1$. As default choice we set $\lambda = 3/4$ and $N_* = 500$, as it also proved to be effective in the simulation study of Section 4.1. Then, we select hyperparameters by minimizing the prequential log-likelihood, obtaining $\delta = (0.45, 0.41)$ for temperature and habitat, respectively, and $\sigma = (3.81, 1.53, 1.12, 1.06)$ for the response. For permutation invariance, we average the MAD predictive and the corresponding prequential log-likelihood over 10

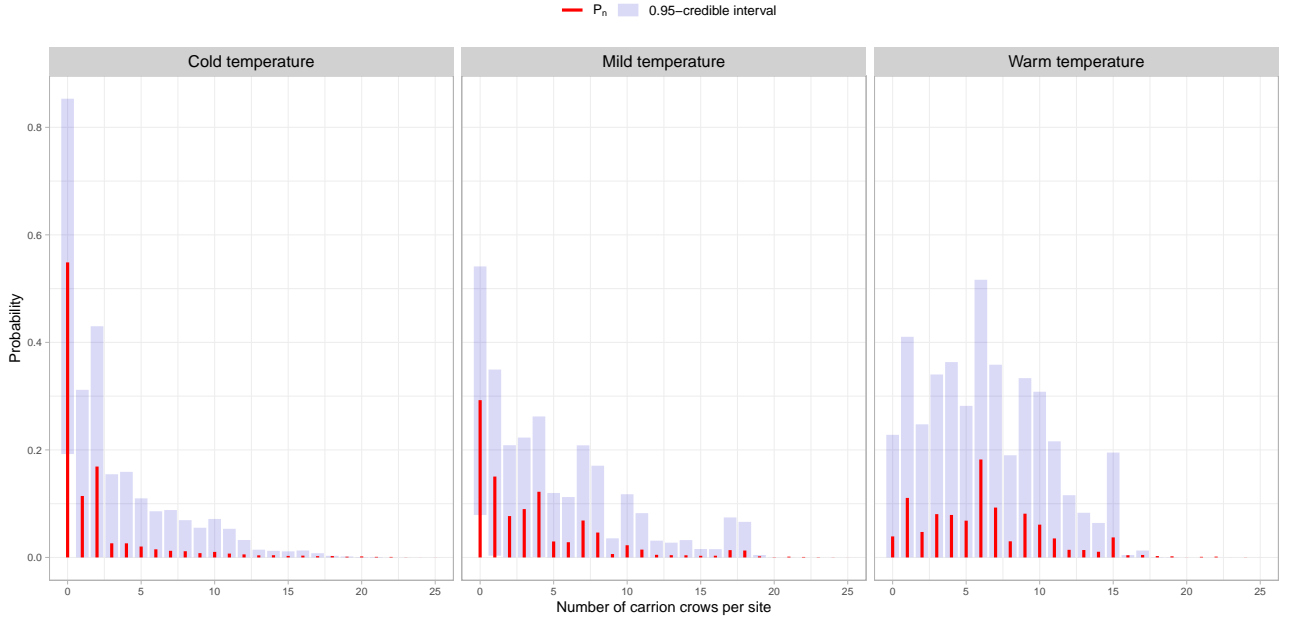


Figure 5: MAD predictive distribution of carrion crows across temperatures (red) with corresponding 0.95 credible interval (blue).

permutations. Computing the MAD predictive distribution averaged over permutations takes 25.68 seconds on a 3.2 GHz 8-Core Apple M1 CPU. Uncertainty quantification is carried out using a predictive resampling algorithm with $N = n + 1000$ and $B = 1000$. To compare methods, we evaluate out-of-sample predictive accuracy using predictive mean squared error (MSE) computed with respect to the data obtained at the same locations for year 2010. As a point estimate for MAD sequences we consider the population mean computed at time n . The MAD sequence had the best predictive performance (MSE = 3.40), followed by GJAM (3.78), GLVM-ZINB (4.69), HMSC (4.70), GLVM-NB (4.72). Moreover, as shown in Appendix C, the MAD sequence performs well in capturing the dependence structure between species. In contrast, popular parametric latent variable models built from elaborations of hierarchical GLMs struggle to recover the empirical dependence structure.

The results obtained using MAD sequences provide valuable insights. The right panel of Figure 4 presents the posterior distribution of the population mean for each species in each urban location, obtained as discussed in Section 2.3. The figure suggests that there are more crows and magpies (95% credible intervals [3.15, 11.28] and [0.70, 8.81], respectively) in urban habitats compared to ravens and jays (95% c.i. [0.06, 1.61] and [0.11, 1.57], respectively). This aligns with Matsyura et al. (2016) and Jokimäki et al. (2022), which indicate that urban settlements serve as stable wintering environments for magpies and crows. As shown in the left panel of Figure 4, there is a positive dependence between these two species (posterior mean for correlation is 0.45, with 95% c.i. [0.24, 0.69]), probably due to

shared habitat preferences. A similar result was observed by [Dupak and Telizhenko \(2023\)](#) for hooded crows (a subspecies of carrion crows) and magpies in Ukraine. Moreover, urban environments are also the preferred habitat for magpies (as reported in [Appendix C](#)), probably because urbanization buffers seasonal variations in climate conditions and food availability ([Benmazouz et al., 2021](#)), facilitating magpies adaptation. However, within the urban environment, Eurasian magpies avoid densely populated areas ([Jokimäki et al., 2017](#)). The differences in the estimated distributions at different temperatures represented in [Figure 5](#) suggest that carrion crows prefer areas with higher temperature, which correspond to the Southern Finland region (see [Appendix C](#)). Finally, consistent with [Madge and Burn \(1994\)](#), our results indicate that the distributions of common ravens and Eurasian jays are homogeneous across different habitats and temperature conditions.

6 DISCUSSION

Our proposed MAD sequences provide a flexible and effective approach for nonparametric modeling of discrete data distributions. We have shown that these sequences implicitly define a prior over the data-generating mechanism which, unlike the DP, can induce positive correlations between nearby values in the support, making MAD sequences appealing in practical applications.

As discussed in [Section 2.4](#), the weight sequence $(w_n)_{n \geq 1}$ plays a dual role, governing both the posterior variability induced by the MAD prior and the learning rate of the associated predictive rule. Although various choices for w_n have been proposed—some of which perform well empirically, as illustrated in [Section 4](#)—none currently guarantees well-calibrated frequentist coverage of posterior credible intervals. While this issue can be addressed in parametric settings ([Fong and Holmes, 2021](#); [Fong and Yiu, 2024a](#)), it remains an open challenge in the context of Bayesian nonparametric predictive inference, representing an important area for future research ([Fortini and Petrone, 2025](#)).

Although MAD sequences have proven effective for modeling multivariate count data, including in regression settings, their performance is likely to degrade in high-dimensional cases due to the curse of dimensionality. A promising direction for future work is to incorporate MAD sequences into more structured models—for example, by using them to define priors over latent parameters. See [Airolidi et al. \(2014\)](#) for a precursor to these ideas. In particular, CID sequences could be employed to model low-dimensional latent variables underlying high-dimensional observations. Interesting next steps include establishing theoretical guarantees for these approaches and ensuring their computational scalability.

ACKNOWLEDGEMENTS

This research was partially supported by the National Institutes of Health (grant ID R01ES035625), by the European Research Council under the European Union's Horizon 2020 research and innovation programme (grant agreement No 856506), by the National Science Foundation (NSF IIS-2426762), and by the Office of Naval Research (N00014-21-1-2510). T.R. acknowledges support of MUR - Prin 2022 - Grant no. 2022CLTYP4, funded by the European Union - Next Generation EU.

A PROOFS

A.1 PRELIMINARY RESULTS

In this Section, we provide useful technical results for some of the later proofs, in particular for the asymptotic results. The following theorems from [Berti et al. \(2013\)](#) are employed in Lemma A.1 for proving the convergence in total variation distance of the sequence of MAD predictive distributions and they are included to make the paper self-contained.

Theorem A.1 (Theorem 1 in [Berti et al., 2013](#)). *Let λ be a σ -finite measure on a Polish space S . Let the sequence $(Y_n)_{n \geq 1}$ be CID with*

$$P_n(\cdot) = \mathbb{P}\{Y_{n+1} \in \cdot \mid Y_1, \dots, Y_n\} \longrightarrow P(\cdot)$$

weakly \mathbb{P} -almost surely. Then, $P \ll \lambda$ \mathbb{P} -a.s. if and only if $\|P_n - P\|_{TV} \rightarrow 0$ \mathbb{P} -a.s. and $P_n \ll \lambda$ for all $n \geq 1$.

Theorem A.2 (Theorem 4 in [Berti et al., 2013](#)). *Suppose $(Y_n)_{n \geq 1}$ is CID and $P_n \ll \lambda$ for every $n \geq 1$, with p_n the density of P_n with respect to λ . Then, $P \ll \lambda$ if and only if, for every compact K such that $\lambda(K) < \infty$, p_n is a function on S uniformly integrable with respect to λ_K \mathbb{P} -almost surely, where $\lambda_K(\cdot) = \lambda(\cdot \cap K)$ is the restriction of λ to K .*

In particular, $P \ll \lambda$ \mathbb{P} -a.s. if, for every compact K such that $\lambda(K) < \infty$, there exists $d > 1$ such that

$$\sup_n \int_K p_n(y)^d d\lambda(y) < \infty \tag{16}$$

\mathbb{P} -a.s. Moreover, for condition (16) to be true, it suffices that

$$\sup_n \mathbb{E} \left\{ \int_K p_n(y)^d d\lambda(y) \right\} < \infty$$

\mathbb{P} -a.s.

Lemma A.1. *Let $(P_n)_{n \geq 1}$ be a sequence of MAD predictive distributions and P its limit distribution. Then, $P_n \rightarrow P$ in total variation \mathbb{P} -almost surely as $n \rightarrow \infty$.*

Proof. From Theorem A.1, $P_n \rightarrow P$ in total variation \mathbb{P} -a.s. if P is absolutely continuous with respect to the counting measure λ . From Theorem A.2, P is absolutely continuous with respect to λ if there exists a $d > 1$ such that

$$\sup_n \mathbb{E} \left\{ \int_K p_n(y)^d d\lambda(y) \right\} < \infty$$

for every compact K such that $\lambda(K) < \infty$, where the expectation is taken with respect to Y_1, \dots, Y_n .

In our case, since $p_n(y) \in [0, 1]$ for every $y \in \mathcal{Y}$ and every $n \geq 0$, we have that

$$\sup_n \mathbb{E} \left\{ \int_K p_n(y)^d d\lambda(y) \right\} = \sup_n \mathbb{E} \left\{ \sum_{y \in \mathcal{Y}} p_n(y)^d \delta_K(y) \right\} \leq |K| < \infty$$

by definition of K . □

Lemma A.2 and A.3 provide the convergence of the MH kernel and its squared expectation, respectively. These results are useful for the proofs of Proposition 1 and 2.

Lemma A.2. *For every $y \in \mathcal{Y}$ and every measurable set A ,*

$$K_n(A \mid y) \longrightarrow K(A \mid y)$$

\mathbb{P} -a.s. as $n \rightarrow \infty$, where $K(A \mid y) = \sum_{x \in A} k(x \mid y)$, with

$$k(x \mid y) = \gamma(x, y)k_*(x \mid y) + \mathbb{1}(x = y) \left[1 - \sum_{z \in \mathcal{Y}} \gamma(z, y)k_*(z, y) \right],$$

$$\gamma(x, y) = \min \left\{ 1, \frac{p(x)k_*(y \mid x)}{p(y)k_*(x \mid y)} \right\}.$$

Proof. By Lemma A.1, $\lim_{n \rightarrow \infty} p_n(y) = p(y)$, \mathbb{P} -a.s., for every $y \in \mathcal{Y}$. Then, for every $x, y \in \mathcal{Y}$,

$$\lim_{n \rightarrow \infty} \gamma_n(x, y) = \lim_{n \rightarrow \infty} \min \left\{ 1, \frac{p_n(x)k_*(y \mid x)}{p_n(y)k_*(x \mid y)} \right\} = \min \left\{ 1, \frac{p(x)k_*(y \mid x)}{p(y)k_*(x \mid y)} \right\} = \gamma(x, y)$$

\mathbb{P} -almost surely. It follows that

$$\begin{aligned} \lim_{n \rightarrow \infty} K_n(A \mid y) &= \lim_{n \rightarrow \infty} \sum_{x \in A} k_n(x \mid y) \\ &= \sum_{x \in A} \lim_{n \rightarrow \infty} \left\{ \gamma_n(x, y)k_*(x \mid y) + \mathbb{1}(x = y) \left[1 - \sum_{z \in \mathcal{Y}} \gamma_n(z, y)k_*(z \mid y) \right] \right\} \\ &= \sum_{x \in A} \left\{ \gamma(x, y)k_*(x \mid y) + \mathbb{1}(x = y) \left[1 - \sum_{z \in \mathcal{Y}} \gamma(z, y)k_*(z \mid y) \right] \right\} \\ &= K(A \mid y). \end{aligned}$$

□

Lemma A.3. *For every $H \geq 1$, all measurable sets A_1, \dots, A_H , and every vector $\mathbf{c} = (c_1, \dots, c_H)$ such that $\|\mathbf{c}\| = 1$,*

$$\mathbb{E} \left\{ \left[\sum_{j=1}^H c_j K_n(A_j \mid Y_{n+1}) \right] \left[\sum_{r=1}^H c_r K_n(A_r \mid Y_{n+1}) \right] \mid Y_{1:n} \right\} \longrightarrow \sum_{j,r=1}^H c_j c_r \left[\sum_{y \in \mathcal{Y}} K(A_j \mid y) K(A_r \mid y) p(y) \right]$$

\mathbb{P} -almost surely for $n \rightarrow \infty$.

Proof. We can write

$$\begin{aligned} &\mathbb{E} \left\{ \left[\sum_{j=1}^H c_j K_n(A_j \mid Y_{n+1}) \right] \left[\sum_{r=1}^H c_r K_n(A_r \mid Y_{n+1}) \right] \mid Y_{1:n} \right\} \\ &= \sum_{y \in \mathcal{Y}} \left[\sum_{j=1}^H c_j K_n(A_j \mid y) \right] \left[\sum_{r=1}^H c_r K_n(A_r \mid y) \right] p_n(y) \\ &= \sum_{j=1}^H \sum_{r=1}^H c_j c_r \left[\sum_{y \in \mathcal{Y}} K_n(A_j \mid y) K_n(A_r \mid y) p_n(y) \right]. \end{aligned}$$

Then, we have that

$$\begin{aligned}
& \left| \sum_{y \in \mathcal{Y}} K_n(A_j | y) K_n(A_r | y) p_n(y) - \sum_{y \in \mathcal{Y}} K(A_j | y) K(A_r | y) p(y) \right| \\
&= \left| \sum_{y \in \mathcal{Y}} K_n(A_j | y) K_n(A_r | y) p_n(y) - \sum_{y \in \mathcal{Y}} K_n(A_j | y) K_n(A_r | y) p(y) \right. \\
&\quad \left. + \sum_{y \in \mathcal{Y}} K_n(A_j | y) K_n(A_r | y) p(y) - \sum_{y \in \mathcal{Y}} K(A_j | y) K(A_r | y) p(y) \right| \\
&\leq \left| \sum_{y \in \mathcal{Y}} K_n(A_j | y) K_n(A_r | y) p_n(y) - \sum_{y \in \mathcal{Y}} K_n(A_j | y) K_n(A_r | y) p(y) \right| \\
&\quad + \left| \sum_{y \in \mathcal{Y}} K_n(A_j | y) K_n(A_r | y) p(y) - \sum_{y \in \mathcal{Y}} K(A_j | y) K(A_r | y) p(y) \right| \\
&\leq \sum_{y \in \mathcal{Y}} K_n(A_j | y) K_n(A_r | y) |p_n(y) - p(y)| + \sum_{y \in \mathcal{Y}} \left| K_n(A_j | y) K_n(A_r | y) - K(A_j | y) K(A_r | y) \right| p(y) \\
&\leq \sum_{y \in \mathcal{Y}} |p_n(y) - p(y)| + \sum_{y \in \mathcal{Y}} \left| K_n(A_j | y) K_n(A_r | y) - K(A_j | y) K(A_r | y) \right| p(y) \\
&\longrightarrow 0 \quad \mathbb{P}\text{-a.s. for } n \rightarrow \infty,
\end{aligned}$$

since the first term converges to zero \mathbb{P} -a.s. because $P_n \rightarrow P$ in L^1 by Lemma A.1 and the second term converges to zero by the dominated convergence theorem because $K_n(A | y) \rightarrow K(A | y)$ by Lemma A.2. \square

Finally, the following Theorems provide the key results for the proof of Proposition 1.

Theorem A.3 (Theorem A1 in Crimaldi, 2009). *On $(\Omega, \mathcal{F}, \mathbb{P})$, for each $n \geq 1$, let $(\mathcal{F}_{n,j})_{j \geq 0}$ be a filtration and $(M_{n,j})_{j \geq 0}$ a real martingale with respect to $(\mathcal{F}_{n,j})_{j \geq 0}$, with $M_{n,0} = 0$, which converges in L^1 to a random variable $M_{n,\infty}$. Set*

$$Z_{n,j} := M_{n,j} - M_{n,j-1} \quad \text{for } j \geq 1, \quad U_n := \sum_{j \geq 1} Z_{n,j}^2, \quad Z_n^* := \sup_{j \geq 1} |Z_{n,j}|.$$

Further, let $(c_n)_{n \geq 1}$ be a sequence of strictly positive integers such that $c_n Z_n^* \rightarrow 0$ \mathbb{P} -a.s. and let \mathcal{U} be a sub-sigma field which is asymptotic for the conditioning system \mathcal{G} defined by $\mathcal{G}_n = \mathcal{F}_{n,c_n}$.

Assume that the sequence $(Z_n^*)_{n \geq 1}$ is dominated in L^1 and that the sequence $(U_n)_{n \geq 1}$ converges almost surely to a positive real random variable U which is measurable with respect to \mathcal{U} . Then, with respect to the conditioning system \mathcal{G} , the sequence $(M_{n,\infty})_{n \geq 1}$ converges to a Gaussian kernel $\mathcal{N}(0, U)$ in the sense of almost sure conditional convergence.

Theorem A.4 (Lemma 4.1 in Crimaldi et al., 2016). *Let $\mathcal{G} = (\mathcal{G}_n)_{n \geq 1}$ be a filtration and $(Z_n)_{n \geq 1}$ be a \mathcal{G} -adapted sequence of real random variables such that $\mathbb{E}\{Z_n | \mathcal{G}_{n-1}\} \rightarrow Z$, \mathbb{P} -a.s. for some random*

variable Z . Moreover, let $(a_n)_{n \geq 1}$ and $(b_n)_{n \geq 1}$ be two positive sequences of strictly positive real numbers such that

$$b_n \uparrow +\infty, \quad \sum_{n \geq 1} (a_n^2 b_n^2)^{-1} \mathbb{E}\{Z_n\} < \infty.$$

Then we have:

i) if $b_n^{-1} \sum_{m=1}^n a_m^{-1} \rightarrow \zeta$ for some constant ζ , then

$$\frac{1}{b_n} \sum_{m=1}^n \frac{Z_m}{a_m} \xrightarrow{a.s.} \zeta Z;$$

ii) if $b_n \sum_{m \geq n} (a_m b_m^2)^{-1} \rightarrow \zeta$ for some constant ζ , then

$$b_n \sum_{m > n} \frac{Z_m}{a_m b_m^2} \xrightarrow{a.s.} \zeta Z;$$

A.2 PROOF OF THEOREM 1

To prove that the MAD sequence $(Y_n)_{n \geq 1}$ is CID, it is sufficient to show that, for all $n \geq 0$ and all measurable sets A ,

$$\mathbb{P}\{Y_{n+2} \in A \mid y_{1:n}\} = \mathbb{P}\{Y_{n+1} \in A \mid y_{1:n}\},$$

which is equivalent to write

$$\mathbb{P}\{Y_{n+2} \in A \mid y_{1:n}\} \equiv \mathbb{E}\{P_{n+1}(A) \mid y_{1:n}\} = P_n(A) \equiv \mathbb{P}\{Y_{n+1} \in A \mid y_{1:n}\}. \quad (17)$$

By rewriting

$$\begin{aligned} \mathbb{E}\{P_{n+1}(A) \mid y_{1:n}\} &= \mathbb{E}\{(1 - w_{n+1})P_n(A) + w_{n+1}K_n(A \mid Y_{n+1}) \mid y_{1:n}\} \\ &= (1 - w_{n+1})P_n(A) + w_{n+1}\mathbb{E}\{K_n(A \mid Y_{n+1}) \mid y_{1:n}\}, \end{aligned}$$

we see that (17) is true if $\mathbb{E}\{K_n(A \mid Y_{n+1}) \mid y_{1:n}\} = P_n(A)$. This is true because

$$\mathbb{E}\{K_n(A \mid Y_{n+1}) \mid y_{1:n}\} = \sum_{t \in A} \sum_{z \in \mathcal{Y}} k_n(t \mid z) p_n(z) \stackrel{(*)}{=} \sum_{t \in A} \sum_{z \in \mathcal{Y}} k_n(z \mid t) p_n(t) = \sum_{t \in A} p_n(t) = P_n(A),$$

for every A and $n \geq 0$, where equivalence $(*)$ is a consequence of the detailed balance condition of MH kernels, that is

$$k_n(z \mid y) p_n(y) = k_n(y \mid z) p_n(z),$$

hence

$$\sum_{z \in \mathcal{Y}} k_n(y \mid z) p_n(z) = \sum_{z \in \mathcal{Y}} k_n(z \mid y) p_n(y) = p_n(y).$$

A.3 PROOF OF COROLLARY 1

- (a) This is a consequence of [Berti et al. \(2004, Theorem 2.5\)](#).
- (b) This is a consequence of [Berti et al. \(2004, Lemma 2.4, Theorem 2.2\)](#).
- (c) Define \mathcal{P} as the space of probability functions on \mathcal{Y} . Let $\Pi(\cdot)$ and $\Pi(\cdot \mid y_{1:n})$ denote the prior and posterior law of P , respectively. Then,

$$\mathbb{E}(\theta) = \mathbb{E}\{P(f)\} = \mathbb{E}\left\{\sum_{y \in \mathcal{Y}} f(y)p(y)\right\} = \sum_{y \in \mathcal{Y}} f(y) \int_{\mathcal{P}} p(y)\Pi(dP) = \sum_{y \in \mathcal{Y}} f(y)p_0(y) = P_0(f) = \theta_0$$

and

$$\begin{aligned} \mathbb{E}(\theta \mid y_{1:n}) &= \mathbb{E}\{P(f) \mid y_{1:n}\} = \mathbb{E}\left\{\sum_{y \in \mathcal{Y}} f(y)p(y) \mid y_{1:n}\right\} \\ &= \sum_{y \in \mathcal{Y}} f(y) \int_{\mathcal{P}} p(y)\Pi(dP \mid y_{1:n}) \\ &= \sum_{y \in \mathcal{Y}} f(y)p_n(y) \\ &= P_n(f) = \theta_n, \end{aligned}$$

where $\int_{\mathcal{P}} p(y)\Pi(dP) = p_0(y)$ and $\int_{\mathcal{P}} p(y)\Pi(dP \mid y_{1:n}) = p_n(y)$ follows because the sequence $(Y_n)_{n \geq 1}$ is CID.

A.4 PROOF OF PROPOSITION 1

The proof specializes the proof of [Fortini and Petrone \(2020, Theorem 7\)](#), which is based on [Theorem A.3](#) and [Theorem A.4](#). By Cramer-Wold device, it is sufficient to show that, for every vector $\mathbf{c} = (c_1, \dots, c_H)$ such that $\|\mathbf{c}\| = 1$ and every $t \in \mathbb{R}$,

$$\mathbb{P}\left\{\sqrt{r_n} \sum_{h=1}^H c_h [P(A_h) - P_n(A_h)] \leq t \mid Y_{1:n}\right\} \longrightarrow \Phi\left\{(\mathbf{c}^\top \Sigma \mathbf{c})^{-1/2} t\right\} \quad (18)$$

\mathbb{P} -almost surely, where $\Phi(\cdot)$ denotes the standard normal cumulative distribution function.

The sequence $(\sum_{h=1}^H c_h P_n(A_h))_{n \geq 1}$ is a bounded martingale converging to $\sum_{h=1}^H c_h P(A_h)$ \mathbb{P} -a.s. in L^1 , as consequence of [Lemma A.1](#). Let

$$M_{n,j} = \sqrt{r_n} \left[\sum_{h=1}^H c_h P_n(A_h) - \sum_{h=1}^H c_h P_{n-j+1}(A_h) \right], \quad \mathcal{F}_{n,j} = Y_{1:n+j-1}$$

for $j \geq 1$ and $M_{n,0} = 0$, $\mathcal{F}_{n,0} = Y_{1:n}$. $(M_{n,j})_{j \geq 0}$ is a zero-mean martingale with respect to the filtration $(\mathcal{F}_{n,j})_{j \geq 1}$ under \mathbb{P} . Let

$$Z_{n,j} := M_{n,j} - M_{n,j-1} = \sqrt{r_n} w_{n+j-1} T_{n+j-1}, \quad U_n := \sum_{j \geq 1} Z_{n,j}^2 = r_n \sum_{j \geq 1} w_{n+j-1}^2 T_{n+j-1}^2, \quad Z_n^* := \sup_{j \geq 1} |Z_{n,j}|,$$

with

$$T_{n+j-1} = \sum_{h=1}^H c_h [P_{n+j-2}(A_h) - K_{n+j-2}(A_h | Y_{n+j-1})].$$

Equation (18) follows from Theorem A.3 if we can show that $(Z_n^*)_{n \geq 1}$ is dominated in L^1 and $(U_n)_{n \geq 1}$ converges \mathbb{P} -a.s. to $\sum_{h,r=1}^H c_h c_r \Sigma_{hr}$. $(Z_n^*)_{n \geq 1}$ is dominated in L^1 because

$$\sup_{j \geq 1} |Z_{n,j}| = \sqrt{r_n} \sup_{j \geq 1} |w_{n+j-1}| |T_{n+j-1}| \leq \sqrt{r_n} \sup_{j \geq 1} |w_{n+j-1}| \longrightarrow 0$$

by assumption. To prove that U_n converges \mathbb{P} -a.s. to $\sum_{h,r=1}^H c_h c_r \Sigma_{hr}$ we employ part *ii*) of Theorem A.4, with

$$b_{m+1} = r_m, \quad a_m = (b_m^2 w_m^2)^{-1}$$

for $m \geq 1$ and $b_1 = r_1$. Then, we can write

$$U_n = b_{n+1} \sum_{s \geq n+1} (a_s b_s^2)^{-1} T_s^2.$$

By Lemma A.3, we have that, \mathbb{P} -a.s.,

$$\begin{aligned} \mathbb{E}\{T_s^2 | Y_{1:s-1}\} &= \mathbb{E}\left\{ \left[\sum_{h=1}^H c_h P_{s-1}(A_h) - \sum_{h=1}^H c_h K_{s-1}(A_h | Y_s) \right] \right. \\ &\quad \times \left. \left[\sum_{r=1}^H c_r P_{s-1}(A_r) - \sum_{r=1}^H c_r K_{s-1}(A_r | Y_s) \right] | Y_{1:s-1} \right\} \\ &= \mathbb{E}\left\{ \sum_{h=1}^H c_h P_{s-1}(A_h) \sum_{r=1}^H c_r P_{s-1}(A_r) + \sum_{h=1}^H c_h K_{s-1}(A_h | Y_s) \sum_{r=1}^H c_r K_{s-1}(A_r | Y_s) \right. \\ &\quad \left. - \sum_{h=1}^H c_h P_{s-1}(A_h) \sum_{r=1}^H c_r K_{s-1}(A_r | Y_s) - \sum_{h=1}^H c_h K_{s-1}(A_h | Y_s) \sum_{r=1}^H c_r P_{s-1}(A_r) \middle| Y_{1:s-1} \right\} \\ &= \mathbb{E}\left\{ \sum_{h=1}^H c_h K_{s-1}(A_h | Y_s) \sum_{r=1}^H K_{s-1}(A_r | Y_s) | Y_{1:s-1} \right\} - \sum_{h=1}^H c_h P_{s-1}(A_h) \sum_{r=1}^H c_r P_{s-1}(A_r) \\ &= \sum_{h,r=1}^H c_h c_r \left[\sum_{y \in \mathcal{Y}} K_{s-1}(A_h | y) K_{s-1}(A_r | y) p_{s-1}(y) - P_{s-1}(A_h) P_{s-1}(A_r) \right] \\ &\longrightarrow \sum_{h,r=1}^H c_h c_r \left[\sum_{y \in \mathcal{Y}} K(A_h | y) K(A_r | y) p(y) - P(A_h) P(A_r) \right] \\ &= \sum_{h,r=1}^H c_h c_r \Sigma_{hr} \end{aligned}$$

for $s \rightarrow \infty$. Moreover, $\sum_{k \geq 1} (a_k^2 w_k^2)^{-1} \mathbb{E}\{T_k^4\} < \infty$ as $\sum_{k \geq 1} (a_k^2 w_k^2)^{-1} = \sum_{k \geq 1} w_k^4 r_k^2 < \infty$ by assumption and $|T_s| \leq |\sum_{h=1}^H c_h| < \infty$. Since, by assumption, $b_{n+1} \sum_{k \geq n+1} (a_k b_k^2)^{-1} = r_n \sum_{k > n} w_k^2 \longrightarrow 1$, then $U_n \rightarrow \sum_{h,r=1}^H c_h c_r \Sigma_{hr}$ \mathbb{P} -a.s. Therefore, for every $t \in \mathbb{R}$, \mathbb{P} -a.s.,

$$\mathbb{P}\left\{ \sqrt{r_n} \sum_{h=1}^H c_h [P(A_h) - P_n(A_h)] \leq t | Y_{1:n} \right\} = \mathbb{P}\{M_{n,\infty} \leq t | Y_{1:n}\} \longrightarrow \Phi\{(\mathbf{c}^\top \Sigma \mathbf{c})^{-1/2} t\}.$$

A.5 PROOF OF PROPOSITION 2

The proof specializes the proof of [Fortini and Petrone \(2025, Proposition 2.6\)](#) for MAD sequences. By the properties of stable convergence and [Proposition 1](#), it is sufficient to show that Σ_n is positive definite for n large and converges to Σ \mathbb{P} -a.s. with respect to the operator norm.

Since Σ is positive definite by assumption, Σ_n is positive definite for n large if Σ_n converges to Σ in the operator norm, which is equivalent to show that

$$\mathbf{c}^\top \Sigma_n \mathbf{c} \longrightarrow \mathbf{c}^\top \Sigma \mathbf{c} \quad (19)$$

\mathbb{P} -a.s. for every $\mathbf{c} = (c_1, \dots, c_H)$ such that $\|\mathbf{c}\| = 1$.

We can write

$$\mathbf{c}^\top \Sigma_n \mathbf{c} = \sum_{j,r=1}^H c_j c_r \left[\sum_{y \in \mathcal{Y}} K_n(A_j | y) K_n(A_r | y) p_n(y) - P_n(A_j) P_n(A_r) \right].$$

Then, [\(19\)](#) follows since

$$\sum_{y \in \mathcal{Y}} K_n(A_j | y) K_n(A_r | y) p_n(y) \longrightarrow \sum_{y \in \mathcal{Y}} K(A_j | y) K(A_r | y) p(y)$$

by [Lemma A.3](#) and

$$P_n(A_j) P_n(A_r) \longrightarrow P(A_j) P(A_r)$$

by [Corollary 1](#), for every $j, r = 1, \dots, H$.

The final result is obtained by applying the analogue of Slutsky Theorem and Cramer-Wold Theorem for stable convergence (see [Fong and Yiu, 2024a](#), Propositions A2 and A3; and [Häusler and Luschgy, 2015](#), Theorem 3.18, Corollaries 3.19 and 6.3).

B COMPARISON WITH THE DISCRETE COPULA UPDATE

Although our updating using MH kernels shares similarities with the copula update proposed by [Fong et al. \(2023\)](#), the two methods also have important differences. Their approach was designed for continuous data, but they proposed a discrete extension ([Fong et al., 2023](#), Section E.1.3). For $y \in \mathcal{Y} \subseteq \mathbb{N}$, the discrete copula update is

$$d_\rho(y, y_n) = 1 - \rho + \rho \frac{\mathbf{1}(y = y_n)}{p_{n-1}(y)},$$

with $\rho \in (0, 1)$. Then, for every $n \geq 1$ and every $y \in \mathcal{Y}$,

$$\begin{aligned} p_n(y) &= \{1 - w_n + w_n d_\rho(y, y_n)\} p_{n-1}(y) \\ &= (1 - w_n) p_{n-1}(y) + w_n \{(1 - \rho) p_{n-1}(y) + \rho \mathbf{1}(y = y_n)\}. \end{aligned}$$

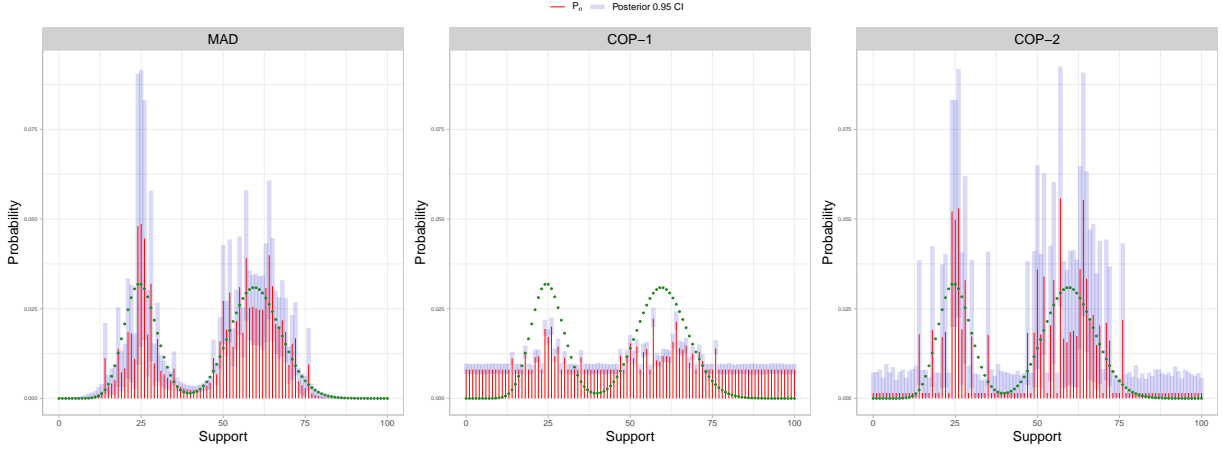


Figure 6: Predictive distributions and 0.95 credible intervals obtained with MAD sequences and two versions of copula updates.

Table 3: Proportion of simulated datasets in which the AUC obtained with COP-A is greater than the one obtained with COP-B.

	$n = 50$	$n = 100$	$n = 150$
$\beta_2 = 0$	0.00	0.00	0.00
$\beta_2 = 0.5$	0.06	0.00	0.02

The induced kernel is a mixture between the old predictive distribution $p_{n-1}(y)$ and a point mass at y_n , with the DP update recovered as $\rho \rightarrow 1$. Therefore, the contribution of the new observation to the update is limited to the assigning of mass $w_n \rho$ to y_n . This structure limits the flexibility of the kernel, as it does not allow the borrowing of information between nearby locations. This is clear from Figure 6, which shows the predictive distribution obtained using the discrete copula update for the illustrative example described in Section 2.5. We employ weights $w_n = (2 - n^{-1})(n + 1)^{-1}$ both for MAD sequence and copula updates. We denote as COP-1 and COP-2 the predictive distributions obtained when ρ is selected by maximizing the corresponding prequential log-likelihood and $\rho = 0.3$, respectively. The former approach produces a small value of $\hat{\rho} = 0.034$, leading to poor learning from the data, too much dependence on the uniform base measure, and small posterior variability. For $\rho = 0.3$, the influence of the base measure is reduced, but the predictive distribution lacks smoothing and posterior variability is large. Conversely, since the MH kernel allows the borrowing of information between nearby values in the support, MAD sequences perform better.

We provide a simulation study to compare copula updates with different variable orderings with MAD sequences. We consider a classification problem with two count covariates. For each sample size $n = \{50, 100, 150\}$, we generate 50 simulated datasets. For each simulation, we sample X_{i1} from the mixture $0.7\text{Poisson}(3) + 0.3\text{Poisson}(12)$, $X_{i2} \sim \text{Poisson}(9)$, and $Y_i \mid x_{i1}, x_{i2} \sim \text{Bin}\{1, \text{logit}^{-1}(\eta_i)\}$, where $\eta_i = 6 - 2.1x_{i1} + \beta_2 x_{i2}$, $i = 1, \dots, n$. We consider settings with $\beta_2 = 0$ – i.e. $X^{(2)}$ is a spurious covariate

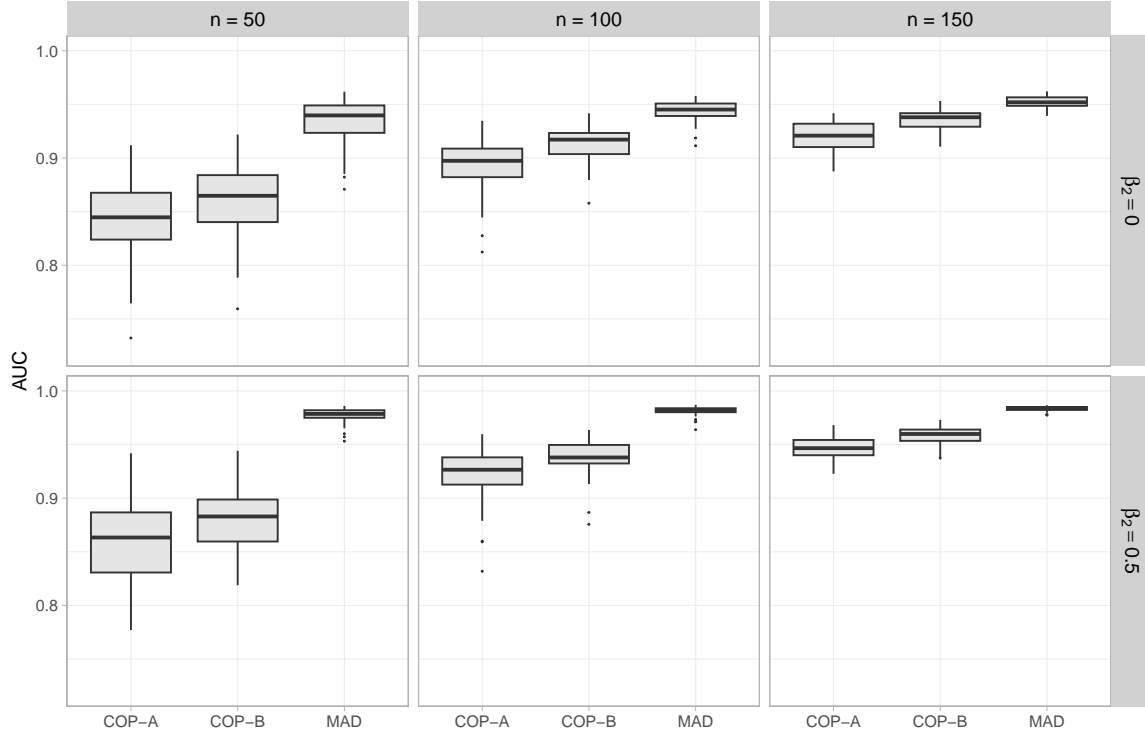


Figure 7: Results of simulation study comparing MAD sequences and two different copula approaches under different data orderings. Box plots show out-of-sample AUC obtained on 10^5 new data points for each scenario.

– and $\beta_2 = 0.5$, respectively. We consider two versions of the copula update, COP-A and COP-B, that sequentially update

$$X_{i1}, \quad X_{i2} \mid x_{i1}, \quad Y_i \mid x_{i1}, x_{i2}, \quad \text{and} \quad X_{i2}, \quad X_{i1} \mid x_{i2}, \quad Y_i \mid x_{i2}, x_{i1},$$

respectively, for $i = 1, \dots, n$. For all methods, we use weights $w_n = (2 - n^{-1})(n + 1)^{-1}$ and select the corresponding hyperparameters by maximizing the prequential log-likelihood. We evaluated the predictive accuracy out of sample using the ROC curve computed on 10^5 new observations and compared the corresponding AUC. As reported in Table 3, COP-B outperforms COP-A in almost every simulated dataset in the six scenarios. This suggests that predictive performance is sensitive to the ordering of predictor variables. As shown in Figure 7, MAD sequences consistently have larger AUC than both versions of the copula update in every scenario.

C ADDITIONAL FIGURES

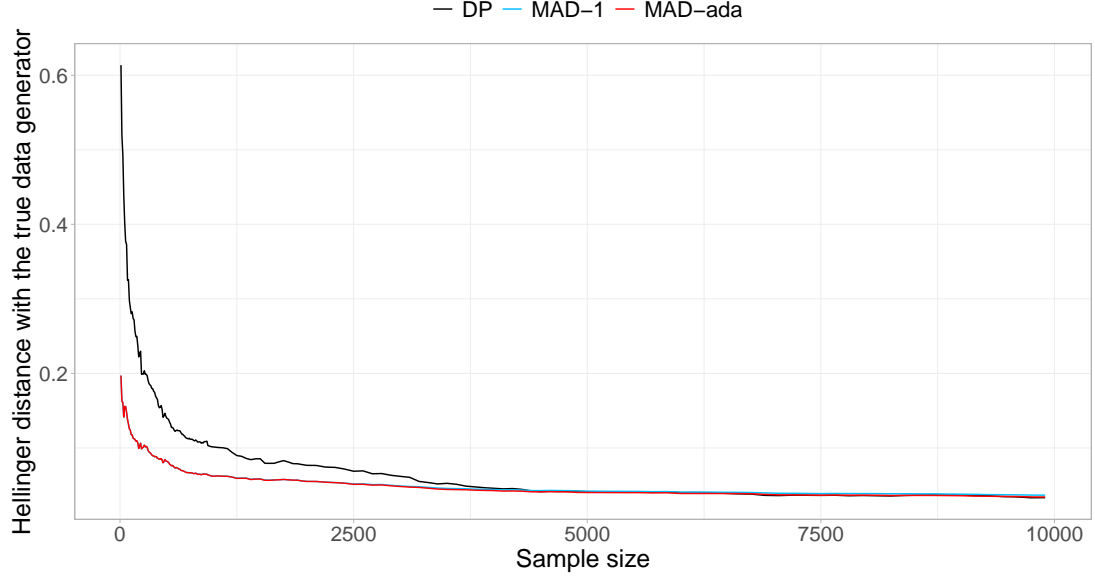


Figure 8: Illustrative example. Hellinger distance of MAD-ada (red), MAD-1 (blue), and DP (black) predictive distributions with respect to the density of the true data generator. Note that MAD-ada and MAD-1 are almost completely overlapping.

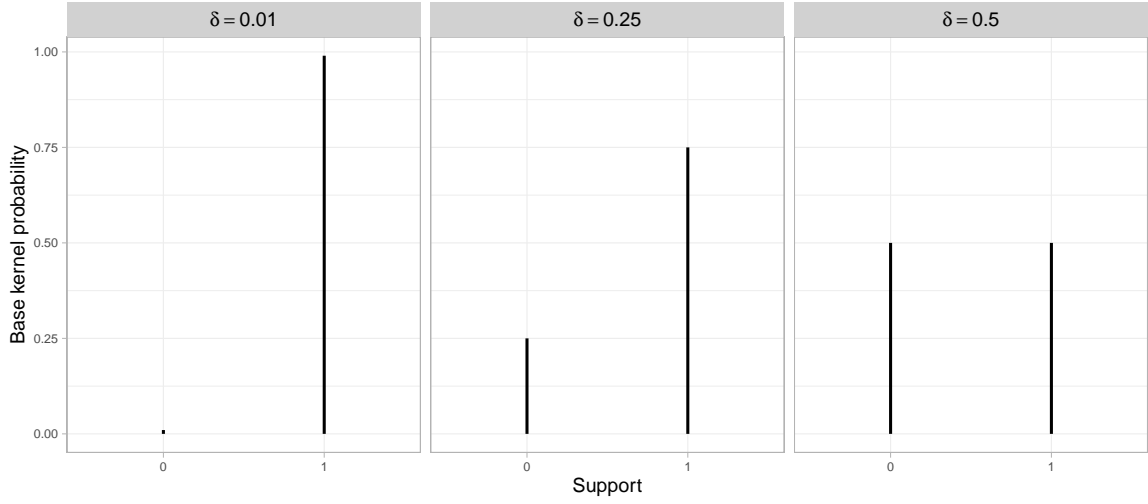


Figure 9: Base kernel for binary data when $y_n = 1$ and $\delta = \{0.01, 0.25, 0.5\}$.

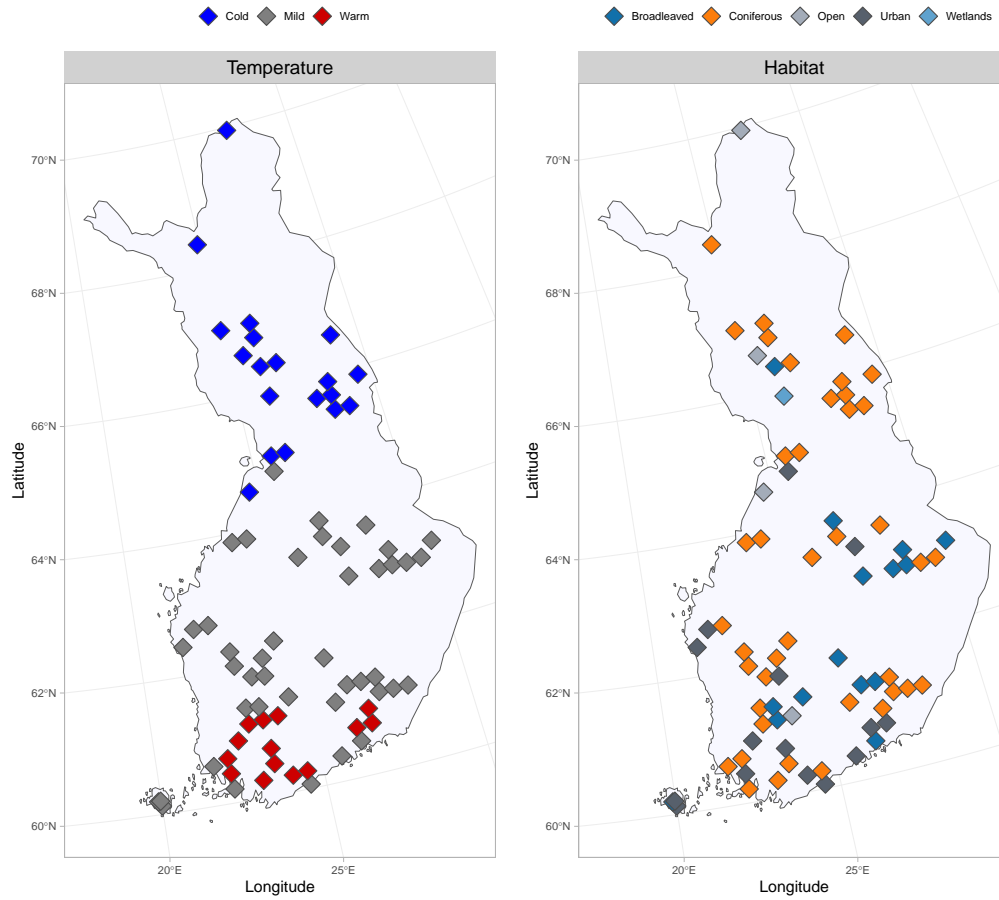


Figure 10: Temperature in April-May (left) and habitat type (right) for each site location.

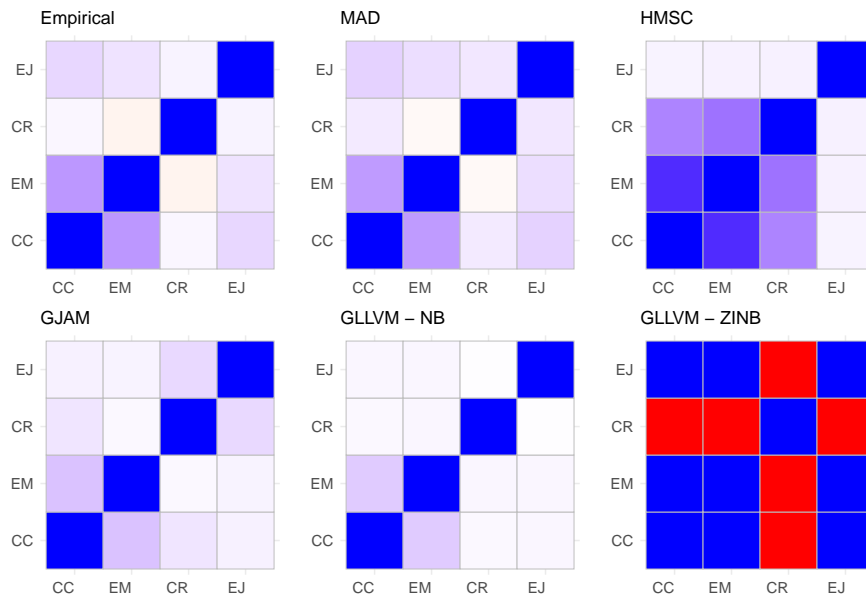


Figure 11: Inferred correlation between corvid species: carrion crow (CC), Eurasian magpie (EM), common raven (CR), and Eurasian jay (EJ). (blue = positive correlation, red = negative correlation, white = zero correlation).

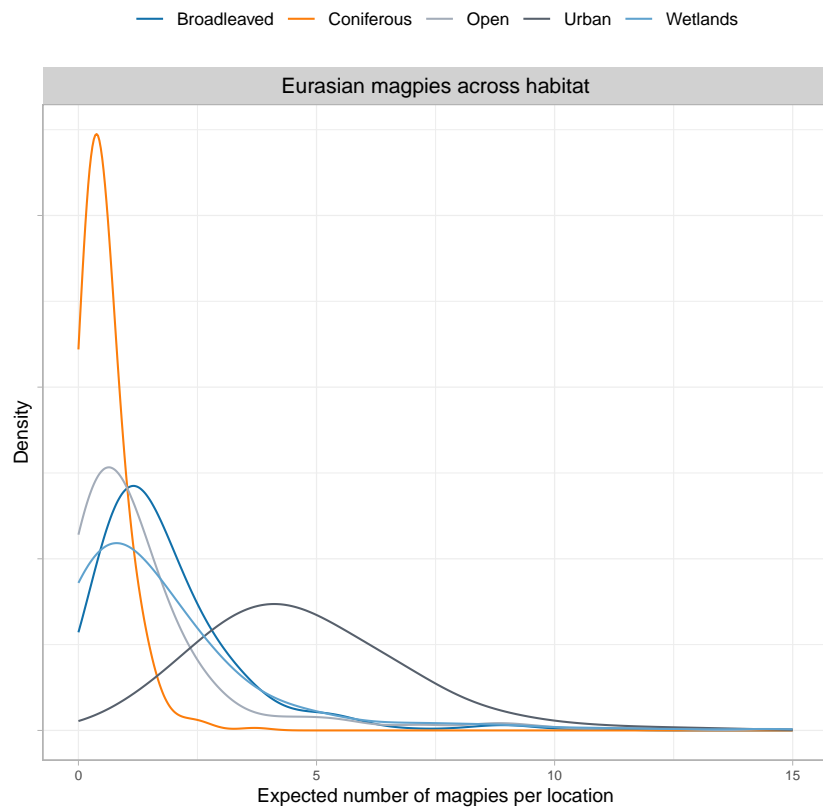


Figure 12: Posterior distribution of the expected number of Eurasian magpies observed at each location in different habitats.

REFERENCES

- Airolidi, E. M., T. Costa, F. Bassetti, F. Leisen, and M. Guindani (2014). Generalized species sampling priors with latent beta reinforcements. *Journal of the American Statistical Association* 109(508), 1466–1480.
- Benmazouz, I., J. Jokimäki, S. Lengyel, L. Juhász, M.-L. Kaisanlahti-Jokimäki, G. Kardos, P. Paládi, and L. Kövér (2021). Corvids in urban environments: A systematic global literature review. *Animals* 11(11), 3226.
- Berti, P., E. Dreassi, F. Leisen, L. Pratelli, and P. Rigo (2023a). Bayesian predictive inference without a prior. *Statistica Sinica* 34(1), 2405–2429.
- Berti, P., E. Dreassi, F. Leisen, L. Pratelli, and P. Rigo (2023b). Kernel based Dirichlet sequences. *Bernoulli* 29(2), 1321–1342.
- Berti, P., E. Dreassi, F. Leisen, L. Pratelli, and P. Rigo (2025). A probabilistic view on predictive constructions for Bayesian learning. *Statistical Science* 40(1), 25–39.
- Berti, P., E. Dreassi, L. Pratelli, and P. Rigo (2021). A class of models for Bayesian predictive inference. *Bernoulli* 27(1), 702–726.
- Berti, P., L. Pratelli, and P. Rigo (2004). Limit theorems for a class of identically distributed random variables. *Annals of Probability* 32(3), 2029–2052.
- Berti, P., L. Pratelli, and P. Rigo (2012). Limit theorems for empirical processes based on dependent data. *Electronic Journal of Probability* 17.
- Berti, P., L. Pratelli, and P. Rigo (2013). Exchangeable sequences driven by an absolutely continuous random measure. *Annals of Probability* 41(3), 2090–2102.
- Bissiri, P. G. and S. G. Walker (2025). Bayesian analysis with conditionally identically distributed sequences. *Electronic Journal of Statistics* 19(1), 1609–1632.
- Blackwell, D. and J. B. MacQueen (1973). Ferguson distributions via Pólya urn schemes. *Annals of Statistics* 1(2), 353–355.
- Canale, A. and D. B. Dunson (2011). Bayesian kernel mixtures for counts. *Journal of the American Statistical Association* 106(496), 1528–1539.
- Canale, A. and I. Prünster (2017). Robustifying Bayesian nonparametric mixtures for count data. *Biometrics* 73(1), 174–184.

- Chipman, H. A., E. I. George, and R. E. McCulloch (2010). Bart: Bayesian additive regression trees. *Annals of Applied Statistics* 4(1), 266–298.
- Clark, J. S., D. Nemergut, B. Seyednasrollah, P. J. Turner, and S. Zhang (2017). Generalized joint attribute modeling for biodiversity analysis: median-zero, multivariate, multifarious data. *Ecological Monographs* 87(1), 34–56.
- Crimaldi, I. (2009). An almost sure conditional convergence result and an application to a generalized Pólya urn. In *International Mathematical Forum*, Volume 4, pp. 1139–1156. Hikari Ltd.
- Crimaldi, I., P. Dai Pra, and I. G. Minelli (2016). Fluctuation theorems for synchronization of interacting Pólya’s urns. *Stochastic processes and their applications* 126(3), 930–947.
- Cui, F. and S. G. Walker (2024). Martingale posterior distributions for log-concave density functions. *arXiv preprint arXiv:2401.14515*.
- Dawid, A. P. (1984). Present position and potential developments: some personal views statistical theory the prequential approach. *Journal of the Royal Statistical Society: Series A (General)* 147(2), 278–290.
- Dupak, V. S. and V. S. Telizhenko (2023). Interactions between hooded crows (*Corvus cornix*) and eurasian magpies (*Pica pica*) and their nesting site preferences in anthropogenic landscapes. *Écoscience* 30(3-4), 210–222.
- Ferguson, T. S. (1973). A Bayesian analysis of some nonparametric problems. *Annals of Statistics* 1(2), 209–230.
- Fong, E. and C. C. Holmes (2021). Conformal Bayesian computation. *Advances in Neural Information Processing Systems* 34, 18268–18279.
- Fong, E., C. C. Holmes, and S. G. Walker (2023). Martingale posterior distributions. *Journal of the Royal Statistical Society Series B: Statistical Methodology* 85(5), 1357–1391.
- Fong, E. and A. Yiu (2024a). Asymptotics for parametric martingale posteriors. *arXiv preprint arXiv:2410.17692*.
- Fong, E. and A. Yiu (2024b). Bayesian quantile estimation and regression with martingale posteriors. *arXiv preprint arXiv:2406.03358*.
- Fortini, S., L. Ladelli, and E. Regazzini (2000). Exchangeability, predictive distributions and parametric models. *Sankhyā: The Indian Journal of Statistics, Series A* 62(1), 86–109.

- Fortini, S. and S. Petrone (2012). Predictive construction of priors in Bayesian nonparametrics. *Brazilian Journal of Probability and Statistics* 26(4), 423–449.
- Fortini, S. and S. Petrone (2020). Quasi-Bayes properties of a procedure for sequential learning in mixture models. *Journal of the Royal Statistical Society Series B: Statistical Methodology* 82(4), 1087–1114.
- Fortini, S. and S. Petrone (2023). Prediction-based uncertainty quantification for exchangeable sequences. *Philosophical Transactions of the Royal Society A* 381(2247), 20220142.
- Fortini, S. and S. Petrone (2025). Exchangeability, prediction and predictive modeling in Bayesian statistics. *Statistical Science* 40(1), 40–67.
- Fortini, S., S. Petrone, and P. Sporysheva (2018). On a notion of partially conditionally identically distributed sequences. *Stochastic Processes and their Applications* 128(3), 819–846.
- Hahn, P. R., R. Martin, and S. G. Walker (2018). On recursive Bayesian predictive distributions. *Journal of the American Statistical Association* 113(523), 1085–1093.
- Häusler, E. and H. Luschgy (2015). *Stable convergence and stable limit theorems*, Volume 74. Springer.
- Hjort, N. L. (1994a). Bayesian approaches to non-and semiparametric density estimation. *Preprint series. Statistical Research Report* <http://urn.nb.no/URN:NBN:no-23420>.
- Hjort, N. L. (1994b). Local Bayesian regression. *Preprint series. Statistical Research Report* <http://urn.nb.no/URN:NBN:no-23420>.
- Holmes, C. C. and S. G. Walker (2023). Statistical inference with exchangeability and martingales. *Philosophical Transactions of the Royal Society A* 381(2247), 20220143.
- Jokimäki, J., M.-L. Kaisanlahti-Jokimäki, and J. Suhonen (2022). Long-term winter population trends of corvids in relation to urbanization and climate at Northern latitudes. *Animals* 12(14), 1820.
- Jokimäki, J., J. Suhonen, T. Vuorisalo, L. Kövér, and M.-L. Kaisanlahti-Jokimäki (2017). Urbanization and nest-site selection of the Black-billed magpie (*Pica pica*) populations in two Finnish cities: From a persecuted species to an urban exploiter. *Landscape and Urban Planning* 157, 577–585.
- Kallenberg, O. (1988). Spreading and predictable sampling in exchangeable sequences and processes. *Annals of Probability* 16(2), 508–534.
- Lindström, Å., M. Green, M. Husby, J. A. Kålås, and A. Lehikoinen (2015). Large-scale monitoring of waders on their boreal and arctic breeding grounds in Northern Europe. *Ardea* 103(1), 3–15.

- Madden, C. F., B. Arroyo, and A. Amar (2015). A review of the impacts of corvids on bird productivity and abundance. *Ibis* 157(1), 1–16.
- Madge, S. and H. Burn (1994). *Crows and jays: a guide to the crows, jays and magpies of the world*. A&C Black.
- Martin, R. and S. T. Tokdar (2009). Asymptotic properties of predictive recursion: robustness and rate of convergence. *Electronic Journal of Statistics* 3, 1455–1472.
- Matsyura, A., K. Jankowski, et al. (2016). Spatial patterns of seasonal distribution of corvidae (the case of urban habitats). *Biosystems Diversity* 24(2), 459–465.
- Mentch, L. and G. Hooker (2016). Quantifying uncertainty in random forests via confidence intervals and hypothesis tests. *Journal of Machine Learning Research* 17(26), 1–41.
- Newton, M. A. (2002). On a nonparametric recursive estimator of the mixing distribution. *Sankhyā: The Indian Journal of Statistics, Series A* 64, 306–322.
- Newton, M. A. and Y. Zhang (1999). A recursive algorithm for nonparametric analysis with missing data. *Biometrika* 86(1), 15–26.
- Ovaskainen, O. and N. Abrego (2020). *Joint species distribution modelling: With applications in R*. Cambridge University Press.
- Ovaskainen, O., N. Abrego, P. Halme, and D. Dunson (2016). Using latent variable models to identify large networks of species-to-species associations at different spatial scales. *Methods in Ecology and Evolution* 7(5), 549–555.
- Rényi, A. (1963). On stable sequences of events. *Sankhyā: The Indian Journal of Statistics, Series A* 25(3), 293–302.
- Sariev, H. and M. Savov (2024). Characterization of exchangeable measure-valued Pólya urn sequences. *Electronic Journal Probability* 29, 1–23.
- Skrondal, A. and S. Rabe-Hesketh (2004). *Generalized latent variable modeling: Multilevel, longitudinal, and structural equation models*. Chapman and Hall/CRC.
- Tikhonov, G., N. Abrego, D. Dunson, and O. Ovaskainen (2017). Using joint species distribution models for evaluating how species-to-species associations depend on the environmental context. *Methods in Ecology and Evolution* 8(4), 443–452.
- Wand, M. P. and M. Jones (1995). *Kernel Smoothing*. Chapman and Hall.